

# Influence of the hexadecapole deformation on the two neutrino double- $\beta$ decay

R Chandra<sup>1,2</sup>, P K Rath<sup>2</sup>, P K Raina<sup>3</sup> and J G Hirsch<sup>4</sup>

<sup>1</sup>Institute of Physics, Sachivalaya Marg, Bhubaneswar-751005, India

<sup>2</sup>Department of Physics, University of Lucknow, Lucknow-226007, India

<sup>3</sup>Department of Physics, IIT Kharagpur-721302, India

<sup>4</sup>Instituto de Ciencias Nucleares, Universidad Nacional Autónoma de México, A.P. 70-543 México 04510 D.F., México

**Abstract.** The two neutrino double beta  $(\beta^-\beta^-)_{2\nu}$  decay of  $^{94,96}\text{Zr}$ ,  $^{98,100}\text{Mo}$ ,  $^{104}\text{Ru}$ ,  $^{110}\text{Pd}$ ,  $^{128,130}\text{Te}$  and  $^{150}\text{Nd}$  nuclei for the  $0^+ \rightarrow 0^+$  transition is studied in the PHFB model in conjunction with the pairing plus quadrupole-quadrupole plus hexadecapole-hexadecapole effective two-body interaction and the effect of the latter is investigated on the calculation of nuclear transition matrix elements  $M_{2\nu}$ . The reliability of the intrinsic wave functions of parent and daughter nuclei involved in the  $(\beta^-\beta^-)_{2\nu}$  decay of above mentioned nuclei is established by obtaining an overall agreement between a number of theoretically calculated spectroscopic properties, namely the yrast spectra, reduced  $B(E2:0^+ \rightarrow 2^+)$  transition probabilities, static quadrupole moments  $Q(2^+)$  and  $g$ -factors  $g(2^+)$  and the available experimental data. The effect of deformation on  $M_{2\nu}$  is also investigated to inveterate its inverse relation with nuclear deformation.

PACS numbers: 23.40.Hc, 21.60.Jz, 23.20.-g, 27.60.+j

## 1. Introduction

The nuclear  $\beta\beta$  decay is a rare second order semi-leptonic transition between two even  $Z$ -even  $N$  isobars  ${}^A_Z X$  and  ${}^A_{Z\pm 2} Y$  involving strangeness conserving charged weak currents. The  $\beta\beta$  decay can be broadly classified into four experimentally distinguishable modes, namely two neutrino double beta  $(\beta\beta)_{2\nu}$  decay [1], neutrinoless double beta  $(\beta\beta)_{0\nu}$  decay [2], single Majoron accompanied neutrinoless double beta  $(\beta\beta\phi)_{0\nu}$  decay [3] and double Majoron accompanied neutrinoless double beta  $(\beta\beta\phi\phi)_{0\nu}$  decay [4]. The  $(\beta\beta)_{2\nu}$  decay conserves the lepton number  $L$  exactly and is an allowed process within the standard model of electroweak unification ( $SM$ ). In  $(\beta\beta)_{0\nu}$  decay, the conservation of lepton number is violated by two units and it is possible in models beyond the  $SM$ , namely GUTs (left-right symmetric  $SO(10)$ ,  $E(6)$  etc.),  $R_p$ -conserving as well as violating SUSY models, leptoquark, compositeness and sterile neutrino scenarios. In fact, the experimental observation of  $(\beta\beta)_{0\nu}$  decay would immediately imply that neutrinos are Majorana particles and all the present experimental activities are directed towards the observation of this particular decay mode. The  $(\beta\beta\phi)_{0\nu}$  and  $(\beta\beta\phi\phi)_{0\nu}$  decay modes are possible processes in nine Majoron models as discussed by Bamert and co-workers [5].

These decay modes can proceed via emission of two electrons ( $\beta^-\beta^-$ ), emission of two positrons ( $\beta^+\beta^+$ ), electron-positron conversion ( $\varepsilon\beta^+$ ) and double electron capture ( $\varepsilon\varepsilon$ ). The latter three are energetically competing modes and we refer to them as  $e^+\beta\beta$  modes. There are 35  $\beta^-\beta^-$  and 34  $e^+\beta\beta$  emitters. Further, the transitions in  $\beta\beta$  decay modes may be from  $0^+ \rightarrow J^+$  states. Presently, the study of  $\beta^-\beta^-$  decay for the  $0^+ \rightarrow 0^+$  transition is the most preferable as the other decay rates are suppressed due to kinematic reasons. However, the study of other decay modes will be of importance in distinguishing the role of different mechanisms involved in  $(\beta\beta)_{0\nu}$  decay once it is observed. Thus, the experimental as well as theoretical study of nuclear  $\beta\beta$  decay is quite wide in scope and has been excellently reviewed over the past years [6-23]. In the present work, we restrict our study to  $(\beta^-\beta^-)_{2\nu}$  decay of  ${}^{94,96}\text{Zr}$ ,  ${}^{98,100}\text{Mo}$ ,  ${}^{104}\text{Ru}$ ,  ${}^{110}\text{Pd}$ ,  ${}^{128,130}\text{Te}$  and  ${}^{150}\text{Nd}$  isotopes for the  $0^+ \rightarrow 0^+$  transition only.

The study of  $(\beta^-\beta^-)_{2\nu}$  decay is quite interesting from the nuclear structure point of view. The  $(\beta^-\beta^-)_{2\nu}$  decay has been experimentally observed in case of ten nuclei namely,  ${}^{48}\text{Ca}$ ,  ${}^{76}\text{Ge}$ ,  ${}^{82}\text{Se}$ ,  ${}^{96}\text{Zr}$ ,  ${}^{100}\text{Mo}$ ,  ${}^{116}\text{Cd}$ ,  ${}^{128,130}\text{Te}$ ,  ${}^{150}\text{Nd}$  and  ${}^{238}\text{U}$  out of 35 possible candidates [24] and one can extract nuclear transition matrix elements (NTMEs) from the observed half-lives. Using the average half-lives [28] and the phase space factors [14], the extracted NTMEs  $M_{2\nu}$  vary from  $0.0152 \pm 0.0008$  ( $0.0238 \pm 0.0013$ ) to  $0.1222 \pm 0.0034$  ( $0.1909 \pm 0.0053$ ) for  $g_A = 1.25$  (1.00) corresponding to  ${}^{130}\text{Te}$  and  ${}^{100}\text{Mo}$  respectively. A comparison between the theoretically calculated and experimentally extracted NTMEs provides a cross-check on the reliability of different nuclear models used for the calculation of NTMEs.

It is observed in all cases of  $(\beta^-\beta^-)_{2\nu}$  decay that the NTMEs  $M_{2\nu}$  are sufficiently quenched. The calculation of  $M_{2\nu}$  requires the knowledge of the  $\beta^-$  or (p, n) amplitude for the initial nucleus and the  $\beta^+$  or (n, p) amplitude of the final nucleus, which in turn requires a complete set of states of the intermediate nucleus in addition to the initial and final nuclear states. The understanding as well as realization of this quenching mechanism is the main motive of all the theoretical calculations. In solving this problem, different nuclear models and nuclear structure scenarios have been applied. Nuclear models, which are used in the calculation of NTMEs of  $(\beta^-\beta^-)_{2\nu}$  decay, can be broadly classified in to shell model and its variants, quasiparticle random phase approximations (QRPA) and extensions to it and alternative models. The details about these models -their advantages as well as limitations- have been discussed by Suhonen and Civitarese [18] and Faessler and Simkovic [19].

The shell-model is the best choice for the calculation of the NTMEs as it attempts to solve the nuclear many-body problem as exactly as possible. The large scale shell model calculations by Caurier *et al.* are more realistic in which  ${}^{76}\text{Ge}$ ,  ${}^{82}\text{Se}$ ,  ${}^{124}\text{Sn}$ ,  ${}^{128}\text{Te}$ ,  ${}^{130}\text{Te}$  and  ${}^{136}\text{Xe}$  have been studied [25]. The  $M_{2\nu}$  of  ${}^{82}\text{Se}$  is calculated exactly and those of  ${}^{76}\text{Ge}$  and  ${}^{136}\text{Xe}$  are dealt in a nearly exact manner [26]. In the QRPA model, Vogel and Zirnbauer were the first to provide an explanation of the observed suppression of  $M_{2\nu}$  by a proper inclusion of ground state correlations through the proton-neutron  $p$ - $p$  interaction in the  $S=1$ ,  $T=0$  channel and the calculated half-lives are in close agreement with all the experimental data [27]. The QRPA frequently overestimates the ground state correlations and to cure the strong suppression of  $M_{2\nu}$  due to increase in the attractive proton-neutron interaction, several extensions of QRPA have been

proposed. The most important proposals are inclusion of proton-neutron pairing, renormalized QRPA, higher QRPA, multiple commutator method (MCM) and particle number projection. However, none of the above methods is free from ambiguities [19]. Alternative models, as the operator expansion method (OEM), the broken SU(4) symmetry, two vacua RPA, the pseudo SU(3) and the single state dominance hypothesis (SSDH) have their own problems [18].

The  $(\beta^-\beta^-)_{0\nu}$  decay has not been experimentally observed hitherto, and only limits on half-lives of  $(\beta^-\beta^-)_{0\nu}$  decay are available. Klapdor and his collaborators have reported the  $(\beta^-\beta^-)_{0\nu}$  decay of  $^{76}\text{Ge}$  in Heidelberg-Moscow experiment [29]. However, it is felt that the reported result needs independent verification by other experiments [30, 23]. The observed half-life limits permit to extract limits on various effective lepton number violating parameters, namely Majorana neutrino mass, coupling of left and right handed weak currents, mass of right handed heavy neutrino, mass of right handed W-boson, intergeneration Yukawa coupling constants of SUSY models, leptoquark coupling constants, compositeness scale, constraint on sterile neutrinos, Majoron coupling constants, VEP and VLI parameters using the theoretically calculated NTMEs of  $(\beta^-\beta^-)_{0\nu}$  decay. In order to get accurate effective lepton number violating parameters, one has to calculate reliable NTMEs for  $(\beta^-\beta^-)_{0\nu}$  decay. In the absence of experimental data, it is difficult to judge the reliability of wave functions involved in the calculation of NTMEs of  $(\beta^-\beta^-)_{0\nu}$  decay. Usually, the reliability of wave functions is tested by reproducing the experimentally extracted NTMEs  $M_{2\nu}$  as both the modes involve same set of initial and final wave functions although the nuclear transition operators are sensitive to different spin-isospin correlations in  $(\beta^-\beta^-)_{2\nu}$  and  $(\beta^-\beta^-)_{0\nu}$  decay modes.

The two main ingredients deciding the structure of nuclei participating in  $\beta\beta$  decay are the pairing and deformation degrees of freedom. The crucial role of deformation on NTMEs  $M_{2\nu}$  has been predicted in the case of  $(\beta^-\beta^-)_{2\nu}$  decay of  $^{100}\text{Mo}$  and  $^{150}\text{Nd}$  [31, 32]. The existence of an inverse correlation between the GT strength and quadrupole moment has been already shown by Auerbach *et al* [33] and Troltenier *et al* [34]. The effect of deformation on the distribution of the Gamow-Teller strength and  $\beta$ -decay properties has been studied using a quasiparticle Tamm-Dancoff approximation (TDA) based on deformed Hartree-Fock (DHF) calculations with Skyrme interactions [35] and in deformed self consistent HF+BCS+QRPA method with Skyrme type interactions [36]. Náchér *et al* [37] have presented a novel method of deducing the deformation of  $N = Z$  nucleus  $^{76}\text{Sr}$ , based on the comparison of the experimental GT strength distribution  $B(GT)$  from its decay with the results of QRPA calculations. A deformed QRPA formalism, using deformed Woods-Saxon potentials and deformed Skyrme Hartree-Fock mean fields, was developed to describe simultaneously the energy distributions of the single- $\beta$  GT strength and the  $(\beta^-\beta^-)_{2\nu}$  decay matrix elements [38]. The deformation effect on the  $(\beta^-\beta^-)_{2\nu}$  decay for ground-state transition of  $^{76}\text{Ge}$  was studied in the framework of the deformed QRPA with separable Gamow-Teller (GT) residual interaction [39].

In the light of above discussions, the Projected Hartree-Fock Bogoliubov (PHFB) model is a convenient choice as an alternative model in which the pairing and deformation degrees of freedom are incorporated on equal footing and the rotational symmetry is restored by projection technique providing wave functions with good angular momentum for the parent and daughter nuclei involved in  $\beta\beta$  decay. However, the PHFB model is unable to provide information about the structure of the intermediate odd-odd nuclei in its present version and hence, on the single  $\beta$  decay rates and the distribution of GT strength. In spite of this limitation, the PHFB model, in conjunction with pairing plus quadrupole-quadrupole ( $PQQ$ ) interaction [40], has been successfully applied to study the  $(\beta^\pm\beta^\pm)_{2\nu}$  decay for the  $0^+ \rightarrow 0^+$  transition where it was possible to describe the lowest excited states of the parent and daughter nuclei along with their electromagnetic transition strengths, as well as to reproduce their measured  $\beta\beta$  decay rates [41, 42, 43]. In the PHFB model, the role of deformation in reproducing realistic NTMEs  $M_{2\nu}$  has also been investigated and it has been observed that there exists an inverse correlation between the latter and the former [41, 42, 43].

In the present work, we add a hexadecapole-hexadecapole interaction term  $V(HH)$  to the standard  $PQQ$  interaction to check the stability of our previous results of  $(\beta^-\beta^-)_{2\nu}$  decay with respect to the change in effective two-body interaction. In variation-after-projection (VAP) framework, the pairing plus quadrupole-quadrupole plus hexadecapole-hexadecapole ( $PQQHH$ ) interaction has been successfully

applied to study the yrast spectra of  $^{68-76}\text{Ge}$ ,  $^{72-78}\text{Se}$ ,  $^{74-82}\text{Kr}$ ,  $^{100-108}\text{Zr}$  and  $^{100-108}\text{Mo}$  isotopes [44]. The present paper is organized as follows. In section 2, we present the theoretical formalism to calculate the NTME  $M_{2\nu}$  in the PHFB model in conjunction with summation method using  $PQQHH$  interaction. The expressions to calculate the spectroscopic properties, specifically, the yrast spectra, reduced  $B(E2:0^+ \rightarrow 2^+)$  transition probabilities, static quadrupole moments  $Q(2^+)$  and  $g$ -factors  $g(2^+)$  are given by Dixit *et al* [45]. The calculated spectroscopic properties of  $^{94,96}\text{Zr}$ ,  $^{94,96,98,100}\text{Mo}$ ,  $^{98,100,104}\text{Ru}$ ,  $^{104,110}\text{Pd}$ ,  $^{110}\text{Cd}$ ,  $^{128,130}\text{Te}$ ,  $^{128,130}\text{Xe}$ ,  $^{150}\text{Nd}$  and  $^{150}\text{Sm}$  nuclei are compared with the observed experimental data in section 3 and there by, we check the ‘‘goodness of wave functions’’. The same wave functions are used to study the  $(\beta^-\beta^-)_{2\nu}$  decay of  $^{94,96}\text{Zr}$ ,  $^{98,100}\text{Mo}$ ,  $^{104}\text{Ru}$ ,  $^{110}\text{Pd}$ ,  $^{128,130}\text{Te}$  and  $^{150}\text{Nd}$  nuclei for the  $0^+ \rightarrow 0^+$  transition and the results are presented in the same section. We also examine the effect of deformation on NTMEs  $M_{2\nu}$  by varying the strength of  $QQHH$  part of the effective two-body interaction in section 3. While presenting the theoretically calculated results using  $PQQHH$  interaction, we also give our previous results [41, 43] for comparison, which were calculated using  $PQQ$  interaction. Finally, we present some concluding remarks in section 4.

## 2. Theoretical framework

The inverse half-life of the  $(\beta^-\beta^-)_{2\nu}$  decay for the  $0^+ \rightarrow 0^+$  transition [9, 10, 13] is given by

$$[T_{1/2}^{2\nu}(0^+ \rightarrow 0^+)]^{-1} = G_{2\nu}|M_{2\nu}|^2 \quad (1)$$

where the phase space factor  $G_{2\nu}$  can be calculated with good accuracy [10, 14] and the nuclear model dependent NTME  $M_{2\nu}$  is written as

$$\begin{aligned} M_{2\nu} &= \sum_N \frac{\langle 0_F^+ || \sigma\tau^+ || 1_N^+ \rangle \langle 1_N^+ || \sigma\tau^+ || 0_I^+ \rangle}{E_N - (E_I + E_F)/2} \\ &= \sum_N \frac{\langle 0_F^+ || \sigma\tau^+ || 1_N^+ \rangle \langle 1_N^+ || \sigma\tau^+ || 0_I^+ \rangle}{E_0 + E_N - E_I} \end{aligned} \quad (2)$$

with

$$E_0 = \frac{1}{2}(E_I - E_F) = \frac{1}{2}Q_{\beta\beta} + m_e \quad (3)$$

To evaluate (2), it is required to sum over all the intermediate  $1_N^+$  states. However, it is not possible to study the structure of odd-odd nuclei in the present version of the PHFB model. Hence, we carry out the summation over the intermediate states by using the summation method given by Civitarese and Suhonen [46]. Using summation method, the  $M_{2\nu}$  is expressed as

$$M_{2\nu} = \frac{1}{E_0} \left\langle 0_F^+ \left| \sum_{\mu} (-1)^{\mu} \Gamma_{-\mu} F_{\mu} \right| 0_I^+ \right\rangle \quad (4)$$

where  $\Gamma_{\mu}$  is given by

$$\Gamma_{\mu} = \sigma_{\mu} \tau^+ \quad (5)$$

and

$$F_{\mu} = \sum_{\lambda=0}^{\infty} \frac{(-1)^{\lambda}}{E_0^{\lambda}} D_{\lambda} \Gamma_{\mu} \quad (6)$$

with

$$D_{\lambda} \Gamma_{\mu} = [H, [H, \dots, [H, \Gamma_{\mu}] \dots]]^{(\lambda \text{ times})} \quad (7)$$

When the GT operator commutes with the effective two-body interaction, the (4) can be further simplified to

$$M_{2\nu} = \sum_{\pi, \nu} \frac{\langle 0_F^+ || \sigma \cdot \sigma\tau^+ \tau^+ || 0_I^+ \rangle}{E_0 + \varepsilon(n_{\pi}, l_{\pi}, j_{\pi}) - \varepsilon(n_{\nu}, l_{\nu}, j_{\nu})} \quad (8)$$

In the case of pseudo-SU(3) model, the GT operator commutes with the two-body interaction [48, 49, 50] and the energy denominator is a well-defined quantity without any free parameter. It has been evaluated exactly for  $(\beta^-\beta^-)_{2\nu}$  [48, 49] and  $(\varepsilon\varepsilon)_{2\nu}$  modes [50] in the pseudo-SU(3) scheme.

In the present work, we use a Hamiltonian with  $PQQHH$  type of effective two-body interaction. The Hamiltonian is explicitly written as

$$H = H_{sp} + V(P) + \zeta_{qq} [V(QQ) + V(HH)] \quad (9)$$

where  $H_{sp}$  denotes the single particle Hamiltonian. The pairing part of the effective two-body interaction  $V(P)$  is given by

$$V(P) = - \left( \frac{G}{4} \right) \sum_{\alpha\beta} (-1)^{j_\alpha + j_\beta - m_\alpha - m_\beta} a_\alpha^\dagger a_{\bar{\alpha}}^\dagger a_{\bar{\beta}} a_\beta \quad (10)$$

where  $\alpha$  denotes the quantum numbers  $(nljm)$  and the state  $\bar{\alpha}$  is same as  $\alpha$  but with the sign of  $m$  reversed. The  $QQ$  part of the effective interaction  $V(QQ)$  is expressed as

$$V(QQ) = - \left( \frac{\chi_2}{2} \right) \sum_{\alpha\beta\gamma\delta} \sum_{\mu} (-1)^\mu \langle \alpha | q_{2\mu} | \gamma \rangle \langle \beta | q_{2-\mu} | \delta \rangle a_\alpha^\dagger a_\beta^\dagger a_\delta a_\gamma \quad (11)$$

where

$$q_{2\mu} = \left( \frac{16\pi}{5} \right)^{1/2} r^2 Y_{2\mu}(\theta, \phi) \quad (12)$$

The  $HH$  part of the effective interaction  $V(HH)$  is given as

$$V(HH) = - \left( \frac{\chi_4}{2} \right) \sum_{\alpha\beta\gamma\delta} \sum_{\nu} (-1)^\nu \langle \alpha | q_{4\nu} | \gamma \rangle \langle \beta | q_{4-\nu} | \delta \rangle a_\alpha^\dagger a_\beta^\dagger a_\delta a_\gamma \quad (13)$$

with

$$q_{4\nu} = r^4 Y_{4\nu}(\theta, \phi) \quad (14)$$

Further,  $\zeta_{qq}$  is an arbitrary parameter and the final results are obtained by setting  $\zeta_{qq} = 1$ . The purpose of introducing it is to study the effect of deformation by varying the strength of effective two-body  $QQHH$  interaction.

The model Hamiltonian used in the present work does not commute with the GT operator. Hence, the energy denominator is not a well-defined quantity. However, the violation of isospin symmetry for the  $QQHH$  part of our model Hamiltonian is negligible as will be evident from the parameters of the two-body interaction given in section 3. Further, the violation of isospin symmetry for the pairing part of the two-body interaction is presumably small. With these assumptions, the NTME  $M_{2\nu}$  of  $(\beta^-\beta^-)_{2\nu}$  decay for the  $0^+ \rightarrow 0^+$  transition in the PHFB model in conjunction with the summation method can be obtained as follows.

In the PHFB model, states with good angular momentum  $\mathbf{J}$  are obtained from the axially symmetric HFB intrinsic state  $|\Phi_0\rangle$  with  $K=0$  using the standard projection technique [51] given by

$$|\Psi_{00}\rangle = \frac{2J+1}{8\pi^2} \int D_{00}^J(\Omega) R(\Omega) |\Phi_0\rangle d\Omega \quad (15)$$

where  $R(\Omega)$  and  $D_{00}^J(\Omega)$  are the rotation operator and the rotation matrix respectively. The axially symmetric HFB intrinsic state  $|\Phi_0\rangle$  can be written as

$$|\Phi_0\rangle = \prod_{im} (u_{im} + v_{im} b_{im}^\dagger b_{i\bar{m}}^\dagger) |0\rangle \quad (16)$$

where the creation operators  $b_{im}^\dagger$  and  $b_{i\bar{m}}^\dagger$  are defined as

$$b_{im}^\dagger = \sum_{\alpha} C_{i\alpha,m} a_{\alpha,m}^\dagger \quad \text{and} \quad b_{i\bar{m}}^\dagger = \sum_{\alpha} (-1)^{l+j-m} C_{i\alpha,m} a_{\alpha,-m}^\dagger \quad (17)$$

Finally, one obtains the expression for the NTME  $M_{2\nu}$  of  $(\beta^-\beta^-)_{2\nu}$  decay for the  $0^+ \rightarrow 0^+$  transition as [41, 43]

$$\begin{aligned}
M_{2\nu} &= \sum_{\pi,\nu} \frac{\langle \Psi_{00}^{J_f=0} | | \sigma \cdot \sigma \tau^+ \tau^+ | | \Psi_{00}^{J_i=0} \rangle}{E_0 + \varepsilon(n_\pi, l_\pi, j_\pi) - \varepsilon(n_\nu, l_\nu, j_\nu)} \\
&= \left[ n_{(Z,N)}^{J_i=0} n_{(Z+2,N-2)}^{J_f=0} \right]^{-1/2} \int_0^\pi n_{(Z,N),(Z+2,N-2)}(\theta) \sum_{\alpha\beta\gamma\delta} \frac{\langle \alpha\beta | \sigma_1 \cdot \sigma_2 \tau^+ \tau^+ | \gamma\delta \rangle}{E_0 + \varepsilon_\alpha(n_\pi, l_\pi, j_\pi) - \varepsilon_\gamma(n_\nu, l_\nu, j_\nu)} \\
&\quad \times \sum_{\varepsilon\eta} \frac{\left( f_{Z+2,N-2}^{(\pi)*} \right)_{\varepsilon\beta} \left( F_{Z,N}^{(\nu)*} \right)_{\eta\delta}}{\left[ \left( 1 + F_{Z,N}^{(\pi)}(\theta) f_{Z+2,N-2}^{(\pi)*} \right) \right]_{\varepsilon\alpha} \left[ \left( 1 + F_{Z,N}^{(\nu)}(\theta) f_{Z+2,N-2}^{(\nu)*} \right) \right]_{\gamma\eta}} \sin\theta d\theta \quad (18)
\end{aligned}$$

where

$$n^J = \int_0^\pi \left[ \det \left( 1 + F^{(\pi)} f^{(\pi)\dagger} \right) \right]^{1/2} \left[ \det \left( 1 + F^{(\nu)} f^{(\nu)\dagger} \right) \right]^{1/2} d_{00}^J(\theta) \sin(\theta) d\theta \quad (19)$$

and

$$n_{(Z,N),(Z+2,N-2)}(\theta) = \left[ \det \left( 1 + F_{Z,N}^{(\nu)} f_{Z+2,N-2}^{(\nu)\dagger} \right) \right]^{1/2} \times \left[ \det \left( 1 + F_{Z,N}^{(\pi)} f_{Z+2,N-2}^{(\pi)\dagger} \right) \right]^{1/2} \quad (20)$$

The  $\pi(\nu)$  represents the proton (neutron) of nuclei involved in the  $(\beta^-\beta^-)_{2\nu}$  decay process. The matrices  $f_{Z,N}$  and  $F_{Z,N}(\theta)$  are given by

$$f_{Z,N} = \sum_i C_{ij\alpha, m_\alpha} C_{ij\beta, m_\beta} (v_{im_\alpha} / u_{im_\alpha}) \delta_{m_\alpha, -m_\beta} \quad (21)$$

$$F_{Z,N}(\theta) = \sum_{m'_\alpha m'_\beta} d_{m_\alpha, m'_\alpha}^{j_\alpha}(\theta) d_{m_\beta, m'_\beta}^{j_\beta}(\theta) f_{j_\alpha m'_\alpha, j_\beta m'_\beta} \quad (22)$$

With the assumption that the difference in single particle energies of protons in the intermediate nucleus and neutrons in the parent nucleus is mainly due to the difference in Coulomb energies, one obtains

$$\varepsilon(n_\pi, l_\pi, j_\pi) - \varepsilon(n_\nu, l_\nu, j_\nu) = \begin{cases} \Delta_C & \text{for } n_\nu = n_\pi, l_\nu = l_\pi, j_\nu = j_\pi \\ \Delta_C + \Delta E_{s.o. \text{ splitting}} & \text{for } n_\nu = n_\pi, l_\nu = l_\pi, j_\nu \neq j_\pi \end{cases}, \quad (23)$$

where the Coulomb energy difference  $\Delta_C$  is given by Bohr and Mottelson as [47].

$$\Delta_C = \frac{0.70}{A^{1/3}} \left[ (2Z+1) - 0.76 \left\{ (Z+1)^{4/3} - Z^{4/3} \right\} \right] \text{ MeV} \quad (24)$$

The numerical calculation of  $M_{2\nu}$  for the nuclei involved in the  $(\beta^-\beta^-)_{2\nu}$  decay involves the setup of matrices  $f_{Z,N}$  and  $F_{Z,N}(\theta)$  given by (21) and (22) at 20 Gaussian quadrature points in the range  $(0, \pi)$  using the results of PHFB calculations, which are summarized by amplitudes  $(u_{im}, v_{im})$  and expansion coefficients  $C_{ij,m}$ . Subsequently, the required NTME is evaluated in a straightforward manner using (18).

It must be underlined that, in the present context, the use of the summation method goes beyond the closure approximation, because each proton-neutron excitation is weighted depending on its spin-flip or non-spin-flip character. The explicit inclusion of the spin-orbit splitting in the energy denominator, (23), implies that it cannot be factorized out of the sum in (2). In this sense, employing the summation method in conjunction with the PHFB formalism is richer than what was done in previous application with the pseudo SU(3) model [48, 49].

### 3. Results and discussions

The model space and single particle energies (SPE's) are the same as in our earlier calculation on  $(\beta^-\beta^-)_{2\nu}$  decay for the  $0^+ \rightarrow 0^+$  transition [41, 43]. However, we briefly discuss in the following the model space and single particle energies (SPE's) used to generate the HFB wave functions for convenience. We treat the doubly even nucleus  $^{76}\text{Sr}$  ( $N = Z = 38$ ) as an inert core in case of  $^{94,96}\text{Zr}$ ,  $^{94,96,98,100}\text{Mo}$ ,  $^{98,100,104}\text{Ru}$ ,  $^{104,110}\text{Pd}$  and  $^{110}\text{Cd}$  nuclei, with the valence space spanned by  $1p_{1/2}$ ,  $2s_{1/2}$ ,  $1d_{3/2}$ ,  $1d_{5/2}$ ,  $0g_{7/2}$ ,  $0g_{9/2}$  and  $0h_{11/2}$  orbits for protons and neutrons. The  $1p_{1/2}$  orbit has been included in the valence space to examine the role of the  $Z = 40$  proton core vis-a-vis the onset of deformation in the highly neutron rich isotopes. The set of single particle energies (SPE's) used here are (in MeV)  $\varepsilon(1p_{1/2}) = -0.8$ ,  $\varepsilon(0g_{9/2}) = 0.0$ ,  $\varepsilon(1d_{5/2}) = 5.4$ ,  $\varepsilon(2s_{1/2}) = 6.4$ ,  $\varepsilon(1d_{3/2}) = 7.9$ ,  $\varepsilon(0g_{7/2}) = 8.4$  and  $\varepsilon(0h_{11/2}) = 8.6$  for proton and neutron.

In case of  $^{128,130}\text{Te}$ ,  $^{128,130}\text{Xe}$ ,  $^{150}\text{Nd}$  and  $^{150}\text{Sm}$  nuclei, we treat the doubly even nucleus  $^{100}\text{Sn}$  ( $N = Z = 50$ ) as an inert core with the valence space spanned by  $2s_{1/2}$ ,  $1d_{3/2}$ ,  $1d_{5/2}$ ,  $1f_{7/2}$ ,  $0g_{7/2}$ ,  $0h_{9/2}$  and  $0h_{11/2}$  orbits for protons and neutrons. The change of model space is forced upon as in the model space used for mass region  $A \approx 100$ , the number of neutrons increase to about 40 for nuclei occurring in the mass region  $A \approx 130$ . With the increase in neutron number, the yrast energy spectra gets compressed due to increase in the attractive part of effective two-body interaction. The set of single particle energies (SPE's) used here are in MeV:  $\varepsilon(1d_{5/2}) = 0.0$ ,  $\varepsilon(2s_{1/2}) = 1.4$ ,  $\varepsilon(1d_{3/2}) = 2.0$ ,  $\varepsilon(0g_{7/2}) = 4.0$ ,  $\varepsilon(0h_{11/2}) = 6.5$  (4.8 for  $^{150}\text{Nd}$  and  $^{150}\text{Sm}$ ),  $\varepsilon(1f_{7/2}) = 12.0$  (11.5 for  $^{150}\text{Nd}$  and  $^{150}\text{Sm}$ ),  $\varepsilon(0h_{9/2}) = 12.5$  (12.0 for  $^{150}\text{Nd}$  and  $^{150}\text{Sm}$ ) for proton and neutron.

The HFB wave functions are generated using an effective Hamiltonian with  $PQQHH$  type of two-body interaction. Explicitly, the Hamiltonian can be written as

$$H = H_{sp} + V(P) + \zeta_{qq} [V(QQ) + V(HH)] \quad (25)$$

where  $H_{sp}$  denotes the single particle Hamiltonian. The  $V(P)$ ,  $V(QQ)$  and  $V(HH)$  represent the pairing, quadrupole-quadrupole and hexadecapole-hexadecapole part of the effective two-body interaction. The  $\zeta_{qq}$  is an arbitrary parameter and the final results are obtained by setting the  $\zeta_{qq} = 1$ . The purpose of introducing  $\zeta_{qq}$  is to study the role of deformation by varying the strength of  $QQ$  interaction. The strengths of the pairing interaction is fixed through the relation  $G_p = 30/A$  MeV and  $G_n = 20/A$  MeV, which are same as used by Heestand *et al.* [52] to explain the experimental  $g(2^+)$  data of some even-even Ge, Se, Mo, Ru, Pd, Cd and Te isotopes in Greiner's collective model [53]. For  $^{94}\text{Zr}$  and  $^{96}\text{Zr}$ , we have used  $G_n = 18/A$  and  $22/A$  MeV respectively. The strengths of the pairing interaction fixed for  $^{128,130}\text{Te}$ ,  $^{128,130}\text{Xe}$ ,  $^{150}\text{Nd}$  and  $^{150}\text{Sm}$  are  $G_p = 35/A$  MeV and  $G_n = 35/A$  MeV.

The strengths of the like particle components of the  $QQ$  interaction are taken as  $\chi_{2pp} = \chi_{2nn} = 0.0105$  MeV  $b^{-4}$ , where  $b$  is oscillator parameter. The strength of proton-neutron ( $pn$ ) component of the  $QQ$  interaction  $\chi_{2pn}$  is varied so as to obtain the spectra of considered nuclei namely  $^{94,96}\text{Zr}$ ,  $^{94,96,98,100}\text{Mo}$ ,  $^{98,100,104}\text{Ru}$ ,  $^{104,110}\text{Pd}$ ,  $^{110}\text{Cd}$ ,  $^{128,130}\text{Te}$ ,  $^{128,130}\text{Xe}$ ,  $^{150}\text{Nd}$  and  $^{150}\text{Sm}$  in optimum agreement with the experimental results. The theoretical spectra has been taken to be the optimum one if the excitation energy of the  $2^+$  state  $E_{2^+}$  is reproduced as closely as possible to the experimental value. The prescribed set of parameters for the strength of  $QQ$  interaction are consistent with those of Arima suggested on the basis of an empirical analysis of effective two-body interaction [54].

The relative magnitudes of the parameters of the  $HH$  part of the two body interaction are calculated from a relation suggested by Bohr and Mottelson [55]. According to them the approximate magnitude of these constants for isospin  $T = 0$  is given by

$$\chi_\lambda = \frac{4\pi}{2\lambda + 1} \frac{m\omega_0^2}{A \langle r^{2\lambda-2} \rangle} \quad \text{for } \lambda = 1, 2, 3, 4 \dots \quad (26)$$

and the parameters for the  $T = 1$  case are approximately half of their  $T = 0$  counterparts. We take the  $\chi_4$  for  $T = 1$  case as exactly half of the  $T = 0$  case. Using  $b = 1.0032A^{1/6}$ , one obtains

$$\begin{aligned} \chi_4 &= \left[ \left( \frac{16}{25} \right) \left( \frac{2}{3} \right)^{2/3} \right] \chi_2 A^{-2/3} b^{-4} \\ &= 0.4884 \chi_2 A^{-2/3} b^{-4} \end{aligned} \quad (27)$$

We fix  $\chi_{2pn}$  through the experimentally available energy spectra for a given model space, SPE's,  $G_p$ ,  $G_n$  and  $\chi_{2pp}$ . We present the values of  $\chi_{2pn}$  in table 1. All these input parameters are kept fixed to calculate other spectroscopic properties. Further, we have performed independent calculations for the parent and daughter nuclei involved in the  $\beta\beta$  decay, whose deformations are in general different.

### 3.1. Yrast spectra and electromagnetic properties

The calculated values of excitation energies  $E_{2^+}$ ,  $E_{4^+}$  and  $E_{6^+}$  for all the nuclei of interest along with the experimental ones [56] are given in table 1. It can be seen from table that the theoretical spectra is more expanded in comparison to the experimental spectra for all nuclei although the agreement between the theoretically calculated and experimentally observed  $E_{2^+}$  is quite good. This can be taken care in conjunction with the VAP prescription [57]. However, our aim is to reproduce the properties of only low-lying  $2^+$  state and hence, we do not invoke the VAP prescription, which will unnecessarily complicate the numerical calculation.

The reduced transition probabilities  $B(E2:0^+ \rightarrow 2^+)$  are calculated for effective charges  $e_{eff} = 0.40, 0.50$  and  $0.60$ . The experimentally observed results [58, 59] are also given in the same table. It is noticed that the calculated and the observed  $B(E2:0^+ \rightarrow 2^+)$  values are in excellent agreement in case of  $^{94}\text{Zr}$ ,  $^{94}\text{Mo}$ ,  $^{104}\text{Ru}$  and  $^{104}\text{Pd}$  isotopes for  $e_{eff} = 0.60$ . For the same  $e_{eff}$ , the theoretically calculated  $B(E2:0^+ \rightarrow 2^+)$  differ by 0.007 and 0.004  $\text{e}^2\text{b}^2$  only from the experimental data for  $^{100}\text{Mo}$  and  $^{100}\text{Ru}$  isotopes. In case of  $^{96}\text{Zr}$ ,  $^{96}\text{Mo}$ ,  $^{110}\text{Cd}$ ,  $^{128,130}\text{Te}$ ,  $^{128,130}\text{Xe}$  and  $^{150}\text{Nd}$  isotopes, the calculated  $B(E2:0^+ \rightarrow 2^+)$  agree with experimentally observed values at  $e_{eff} = 0.50$ . However, the calculated  $B(E2:0^+ \rightarrow 2^+)$  differ by 0.056 and 0.508  $\text{e}^2\text{b}^2$  from the experimental results in case of  $^{110}\text{Pd}$  and  $^{150}\text{Sm}$  nuclei for  $e_{eff} = 0.50$ . The calculated  $B(E2:0^+ \rightarrow 2^+)$  of  $^{98}\text{Mo}$  and  $^{98}\text{Ru}$  nuclei for  $e_{eff} = 0.40$  are in agreement with the experimental values.

The theoretically calculated  $Q(2^+)$ , which are calculated for the same effective charges, i.e.  $e_{eff} = 0.40, 0.50$  and  $0.60$ , and the experimental  $Q(2^+)$  results [60] are given in the same table 2. No experimental  $Q(2^+)$  result is available for  $^{94,96}\text{Zr}$  and  $^{128,130}\text{Xe}$  nuclei. For the same effective charge as used in case of  $B(E2:0^+ \rightarrow 2^+)$ , the agreement between the calculated and experimental  $Q(2^+)$  is good for  $^{104}\text{Ru}$ ,  $^{110}\text{Pd}$  and  $^{150}\text{Sm}$  nuclei. The calculated  $Q(2^+)$  are off by 0.10, 0.135, 0.02 and 0.021 eb in case of  $^{98,100}\text{Mo}$ ,  $^{100}\text{Ru}$  and  $^{150}\text{Nd}$  nuclei respectively from the experimental values. The theoretical  $Q(2^+)$  results are quite off from the observed values for the rest of nuclei.

The gyromagnetic factors  $g(2^+)$  are calculated with  $g_l^\pi = 1.0$ ,  $g_l^\nu = 0.0$  and  $g_s^\pi = g_s^\nu = 0.60$  and presented in table 2 along with the available experimental  $g(2^+)$  data [60]. No experimental result is available for  $^{96}\text{Zr}$  and  $^{94,96}\text{Mo}$ . The theoretical  $g(2^+)$  value of  $^{94}\text{Zr}$  is a pathological case. The calculated  $g(2^+)$  is 0.112 nm while the most recent measured value is  $-0.329 \pm 0.015$  nm [61]. The calculated and experimentally observed  $g(2^+)$  results are in good agreement for  $^{98,100}\text{Mo}$ ,  $^{98}\text{Ru}$ ,  $^{104}\text{Pd}$ ,  $^{110}\text{Cd}$  and  $^{128}\text{Xe}$  nuclei. The discrepancy between calculated and experimentally observed  $g(2^+)$  values are 0.047, 0.015, 0.089 and 0.028 nm only for  $^{100,104}\text{Ru}$ ,  $^{110}\text{Pd}$  and  $^{130}\text{Xe}$  nuclei respectively. The theoretically calculated and experimentally observed  $g(2^+)$  results are off by 0.136, 0.257, 0.161 and 0.161 nm in case of  $^{128,130}\text{Te}$ ,  $^{150}\text{Nd}$  and  $^{150}\text{Sm}$  nuclei respectively.

It is observed from table 1 and table 2 that the calculated yrast spectra, reduced  $B(E2:0^+ \rightarrow 2^+)$  transition probabilities, static quadrupole moments  $Q(2^+)$  and gyromagnetic factors  $g(2^+)$  with  $PQQ$  and  $PQQHH$  type of effective two body interaction do not differ much. This establishes the stability of our previous results [41, 43] against the change in effective two-body interaction.

### 3.2. Results of $(\beta^-\beta^-)_{2\nu}$ decay

For the calculation of  $(\beta^-\beta^-)_{2\nu}$  decay rates, the phase space factors  $G_{2\nu}$  of  $^{94,96}\text{Zr}$ ,  $^{98,100}\text{Mo}$ ,  $^{104}\text{Ru}$ ,  $^{110}\text{Pd}$ ,  $^{128,130}\text{Te}$  and  $^{150}\text{Nd}$  nuclei for the  $0^+ \rightarrow 0^+$  transition are  $2.304 \times 10^{-21} \text{ yr}^{-1}$ ,  $1.927 \times 10^{-17} \text{ yr}^{-1}$ ,  $9.709 \times 10^{-29} \text{ yr}^{-1}$ ,  $9.434 \times 10^{-18} \text{ yr}^{-1}$ ,  $9.174 \times 10^{-21} \text{ yr}^{-1}$ ,  $3.984 \times 10^{-19} \text{ yr}^{-1}$ ,  $8.475 \times 10^{-22} \text{ yr}^{-1}$ ,  $4.808 \times 10^{-18} \text{ yr}^{-1}$  and  $1.189 \times 10^{-16} \text{ yr}^{-1}$  respectively for  $g_A = 1.25$  [14]. However, it is more justified to use the nuclear matter value of  $g_A$  around 1.0 in heavy nuclei. Hence, the experimental  $M_{2\nu}$  as well as the theoretical  $T_{1/2}^{2\nu}$  are calculated for  $g_A = 1.0$  and 1.25. In table 3, we compile all the available

experimental and the theoretical results along with our calculated  $M_{2\nu}$  and corresponding half-lives  $T_{1/2}^{2\nu}$  of all the nuclei under consideration for the  $0^+ \rightarrow 0^+$  transition. We also present the  $M_{2\nu}$  extracted from the experimentally observed  $T_{1/2}^{2\nu}$  using the given phase space factors. We present only the theoretical  $T_{1/2}^{2\nu}$  for those models for which no direct or indirect information about  $M_{2\nu}$  is available to us.

The  $(\beta^-\beta^-)_{2\nu}$  decay of  $^{94}\text{Zr}$  for the  $0^+ \rightarrow 0^+$  transition has been investigated experimentally only by Arnold *et al* [62] and the reported limit is  $T_{1/2}^{2\nu} > 1.1 \times 10^{17}$  yr. The half-life calculated in the PHFB model for  $g_A = 1.25$  is  $1.086 \times 10^{23}$  yr, which lies within the range given by Bobyk *et al* [63]. The calculated half-life  $T_{1/2}^{2\nu}$  in QRPA model [65] is smaller than the presently calculated  $T_{1/2}^{2\nu}$  by a factor of 1.5 approximately for  $g_A = 1.25$ . On the other hand, the half-life  $T_{1/2}^{2\nu}$  calculated in OEM [64] is larger than our PHFB model value for  $g_A = 1.25$  by a factor of 15 approximately. The predicted  $T_{1/2}^{2\nu}$  for  $g_A = 1.0$  in the PHFB model is  $2.652 \times 10^{23}$  yr.

In the case of  $^{96}\text{Zr} \rightarrow ^{96}\text{Mo}$ , the theoretically calculated  $M_{2\nu}$  given by Stoica using SRPA [73] is too small in comparison to the NTME extracted from the experimental data. On the other hand, the calculated half-life  $T_{1/2}^{2\nu}$  in the OEM [64] is quite off from the observed experimentally observed result. The  $M_{2\nu}$  calculated by Engel *et al* [74] and Barabash *et al* [72] using QRPA are close to the experimentally observed lower limit of Wieser *et al* [67] for  $g_A = 1.0$ . The  $T_{1/2}^{2\nu}$  calculated by in RQRPA using WS basis and AWS basis [71] are  $4.2 \times 10^{19}$  yr and  $4.4 \times 10^{19}$  yr respectively and agree with the experimental  $T_{1/2}^{2\nu}$  of Kawashima *et al* [69]. The  $T_{1/2}^{2\nu}$  predicted by Staudt *et al* [65] is in agreement with the experimental results of Barabash [68] and Wieser *et al* [67]. The experimentally observed  $T_{1/2}^{2\nu}$  given by NEMO 3 [66] and Wieser *et al* [67] are favored by the  $T_{1/2}^{2\nu}$  calculated in the PHFB model and  $\text{SU}(4)_{\sigma\tau}$  [70] for  $g_A = 1.25$ . The predicted half-life  $T_{1/2}^{2\nu}$  of Bobyk *et al* [63] has a wide range and cover all the available experimental results.

No experimental result for  $T_{1/2}^{2\nu}$  of  $^{98}\text{Mo}$  isotope is available so far. It has been studied theoretically in the QRPA [65], OEM [64] and SRQRPA [63]. The presently calculated  $T_{1/2}^{2\nu} = 6.36 \times 10^{29} - 1.552 \times 10^{30}$  yr for  $g_A = 1.25 - 1.0$  respectively is within the range given by SRQRPA model. The calculated  $T_{1/2}^{2\nu}$  in QRPA and OEM are larger than our predicted value for  $g_A = 1.0$  by approximately a factor of 2 and 4 respectively.

In the case of  $^{100}\text{Mo}$ , the theoretically calculated  $M_{2\nu}$  in SRPA [73] is too small in comparison to the experimental  $M_{2\nu}$ . The  $(\beta^-\beta^-)_{2\nu}$  decay rate of  $^{100}\text{Mo}$  calculated by Staudt *et al* in QRPA [65] and Hirsch *et al* in OEM [64] are off from the experimental  $T_{1/2}^{2\nu}$ . The calculated  $M_{2\nu}$  by Griffiths *et al* [31] using QRPA model favors the results of INS Baksan [84] and LBL [81] for  $g_A = 1.0$ . On the other hand, the  $M_{2\nu}$  predicted by Engel *et al* [74] and Civitarese *et al* [86] are in agreement with the results of LBL [81], LBL collaboration [79], UC Irvine [78] and ITEP+INFN [77] for  $g_A = 1.0$ . The NTMEs  $M_{2\nu}$  predicted in  $\text{SU}(4)_{\sigma\tau}$  [70] and pseudo-SU3 using spherical occupation wave functions [49] are nearly identical and close to the experimental result given by INS Baksan and ITEP+INFN for  $g_A = 1.25$ . The same two  $M_{2\nu}$  are in agreement with the results of UC-Irvine [83], ELEGANTS V, LBL and NEMO 3 for  $g_A = 1.0$ . Further, the NTME  $M_{2\nu}$  given in the PHFB model, QRPA [32] and pseudo-SU3 using deformed occupation wave functions [49] favor the results of UC-Irvine [83], ELEGANTS V, LBL, LBL collaboration and ITEP+INFN for  $g_A = 1.25$ . The results of SSDH [85] are in agreement with the experimental half-lives of LBL, LBL collaboration, UC-Irvine [78] and ITEP+INFN. The decay rate  $T_{1/2}^{2\nu}$  calculated by Bobyk *et al* [63] is in agreement with all the experimental results due to a large range of values.

The  $(\beta^-\beta^-)_{2\nu}$  decay of  $^{104}\text{Ru} \rightarrow ^{104}\text{Pd}$  for the  $0^+ \rightarrow 0^+$  transition has not been experimentally investigated so far. The half-life  $T_{1/2}^{2\nu}$  has been calculated theoretically in QRPA [65] and OEM [64]. Our predicted  $T_{1/2}^{2\nu}$  for  $g_A = 1.25$  is approximately 3.7 times larger than that of calculated in QRPA and smaller than the half-life predicted in OEM by a factor of approximately 1.3. The predicted  $T_{1/2}^{2\nu}$  for  $g_A = 1.0$  in the PHFB model is  $5.73 \times 10^{22}$  yr.

In 1952, Winter had studied the  $(\beta^-\beta^-)_{2\nu}$  decay of  $^{110}\text{Pd}$  isotope for the  $0^+ \rightarrow 0^+$  transition [87].

The deduced half-life limit was  $T_{1/2}^{2\nu} > 6.0 \times 10^{16}$  yr for  $(\beta^-\beta^-)_{2\nu}$  decay mode and  $T_{1/2}^{2\nu} > 6.0 \times 10^{17}$  yr for all modes. Since then, no experiment has been attempted to study the  $\beta^-\beta^-$  decay of  $^{110}\text{Pd}$ . The  $(\beta^-\beta^-)_{2\nu}$  decay of  $^{110}\text{Pd}$  has been studied theoretically in QRPA [65], OEM [64], SRPA [89] and SSDH [86, 88]. The calculated  $T_{1/2}^{2\nu}$  for  $g_A = 1.25$  in the present PHFB model is  $1.74 \times 10^{20}$  yr, which is close to that of Semenov *et al* [88] and approximately twice of Civitarese *et al* [86]. On the other hand, the calculated half-life in SRPA is about 7 times larger than the presently calculated  $T_{1/2}^{2\nu}$  for the same  $g_A$ . The calculated half-life are  $1.16 \times 10^{19}$  yr and  $1.24 \times 10^{21}$  yr in QRPA and OEM respectively. The predicted half-life in the present work for  $g_A = 1.0$  is  $T_{1/2}^{2\nu} = 4.24 \times 10^{20}$  yr.

In the case of  $^{128}\text{Te}$  nucleus, the presently calculated  $M_{2\nu}$  is close to the NTME extracted from the experiments of Takaoka *et al* [90], Manuel [92] and Barabash [28] for  $g_A = 1.0$  while it is close to those of Lin *et al* [93] and Manuel [94] for  $g_A = 1.25$ . The NTMEs  $M_{2\nu}$  calculated in  $\text{SU}(4)_{\sigma\tau}$  [70], SSDH [88] and MCM [95] differ from the presently calculated  $M_{2\nu}$  by factor of 1.4 – 1.6 and are in agreement with the experimental NTMEs due to Lin *et al* [93] and Manuel [94] for  $g_A = 1.0$ . The NTME  $M_{2\nu}$  calculated in SSDH [86] is close to the experimental  $M_{2\nu}$  of Takaoka *et al* [90], Bernatovicz *et al* [91] and Barabash [28] for  $g_A = 1.25$ . The presently calculated  $M_{2\nu}$  is smaller than those calculated in QRPA [74] and WCSM [9] by factor of approximately 2.2 and 3.6 respectively while larger by a factor of approximately 5.5 and 2.5 than the NTMEs calculated in SRPA [89] and SSDH [86] respectively. The half-life  $T_{1/2}^{2\nu}$  calculated in QRPA [65] is close to the experimental  $T_{1/2}^{2\nu}$  due to Lin *et al* [93] and Barabash [28]. The calculated half-lives  $T_{1/2}^{2\nu}$  by Hirsch *et al* in OEM [64] and Scholten *et al* in IBM [96] are quite small. In the PHFB model, the predicted half-life  $T_{1/2}^{2\nu}$  is  $(1.10 - 2.68) \times 10^{24}$  yr for  $g_A = (1.25 - 1.0)$ .

In the PHFB model, the calculated NTME  $M_{2\nu}$  for the  $(\beta^-\beta^-)_{2\nu}$  decay of  $^{130}\text{Te}$  is in agreement with the NTME extracted from the Milano+INFN experiment [97] for  $g_A = 1.0$ , theoretical  $M_{2\nu}$  calculated in the shell model [25] and MCM [95]. The calculated NTME  $M_{2\nu}$  in SRPA [89] is in agreement with the experimental  $M_{2\nu}$  [93, 90, 97] for  $g_A = 1.25$ . The presently calculated  $M_{2\nu}$  is smaller by a factor of approximately 1.5 than those calculated in  $\text{SU}(4)_{\sigma\tau}$  [70] and QRPA [74]. The  $M_{2\nu}$  calculated in RQRPA [71] is close to the experimental NTME of Bernatovicz *et al* [91] for  $g_A = 1.25$ . The calculated half-lives  $T_{1/2}^{2\nu}$  in OEM [64], IBM [96] and WCSM [9] are quite small while the half-life  $T_{1/2}^{2\nu}$  calculated in  $\text{SU}(4)_{\sigma\tau}$  [98] is close to the experimentally observed half-lives [90, 93, 97]. The predicted half-life  $T_{1/2}^{2\nu}$  in the PHFB model is  $(2.10 - 5.13) \times 10^{20}$  yr for  $g_A = (1.25 - 1.0)$ .

In the case of  $^{150}\text{Nd}$  isotope, the calculated  $M_{2\nu}$  in the PHFB model is in agreement with the extracted NTME from NEMO 3 [66] project for  $g_A = 1.25$ . The NTME  $M_{2\nu}$  calculated in pseudo- $\text{SU}(3)$  [48] is close to the experimental  $M_{2\nu}$  of NEMO 3 [66] for  $g_A = 1.0$ . The calculated  $M_{2\nu}$  in  $\text{SU}(4)_{\sigma\tau}$  [70] is larger by a factor of 2.4 than the present value. The half-life  $T_{1/2}^{2\nu}$  calculated in OEM [64] is close to the experimental result of ITEP+INR project while the calculated  $T_{1/2}^{2\nu}$  in QRPA [65] favors the UCI experiment [78]. The calculated half-life  $T_{1/2}^{2\nu}$  in the PHFB model is  $(1.19 - 2.92) \times 10^{19}$  yr for  $g_A = (1.25 - 1.0)$ .

In all the cases discussed in table 3, it turns out that the NTMEs  $M_{2\nu}$  calculated with  $PQQHH$  and  $PQQ$  effective two-body effective interactions are very close. Further, it is noticed that although the calculated spectroscopic properties in the PHFB model for nuclei in the vibrational limit are not in agreement with the experimental data as expected, the calculated NTME  $M_{2\nu}$  of  $^{96}\text{Zr}$  for example is in good agreement with the experimentally observed data.

### 3.3. Deformation effect

To understand the role of deformation on the NTMEs  $M_{2\nu}$ , we investigate its variation with respect to the change in strength of the  $QQHH$  interaction  $\zeta_{qq}$ . The results are presented in figure 1. In all cases, it is observed that NTMEs  $M_{2\nu}$  remain almost constant as the strength of  $\zeta_{qq}$  is changed from 0.0 to 0.6 except in case of  $^{94}\text{Zr}$  and  $^{100}\text{Mo}$  isotopes, where  $M_{2\nu}$  remains almost constant for the variation of  $\zeta_{qq}$  from 0.0 to 0.8. As  $\zeta_{qq}$  is further increased up to 1.5, the NTME  $M_{2\nu}$  starts decreasing except a few anomalies. The experimental  $M_{2\nu}$  is available for  $(\beta^-\beta^-)_{2\nu}$  decay of  $^{96}\text{Zr}$ ,  $^{100}\text{Mo}$ ,  $^{128,130}\text{Te}$  and  $^{150}\text{Nd}$

isotopes. It is noteworthy that the  $M_{2\nu}$  tends to be realistic as  $\zeta_{qq}$  acquires a physical value around 1.0. This suggest that the deformations of the HFB intrinsic states play an important role in reproducing a realistic  $M_{2\nu}$ . Further, it is observed in general that there is an anti-correlation between the NTME  $M_{2\nu}$  and the deformation parameter  $\beta_2$ .

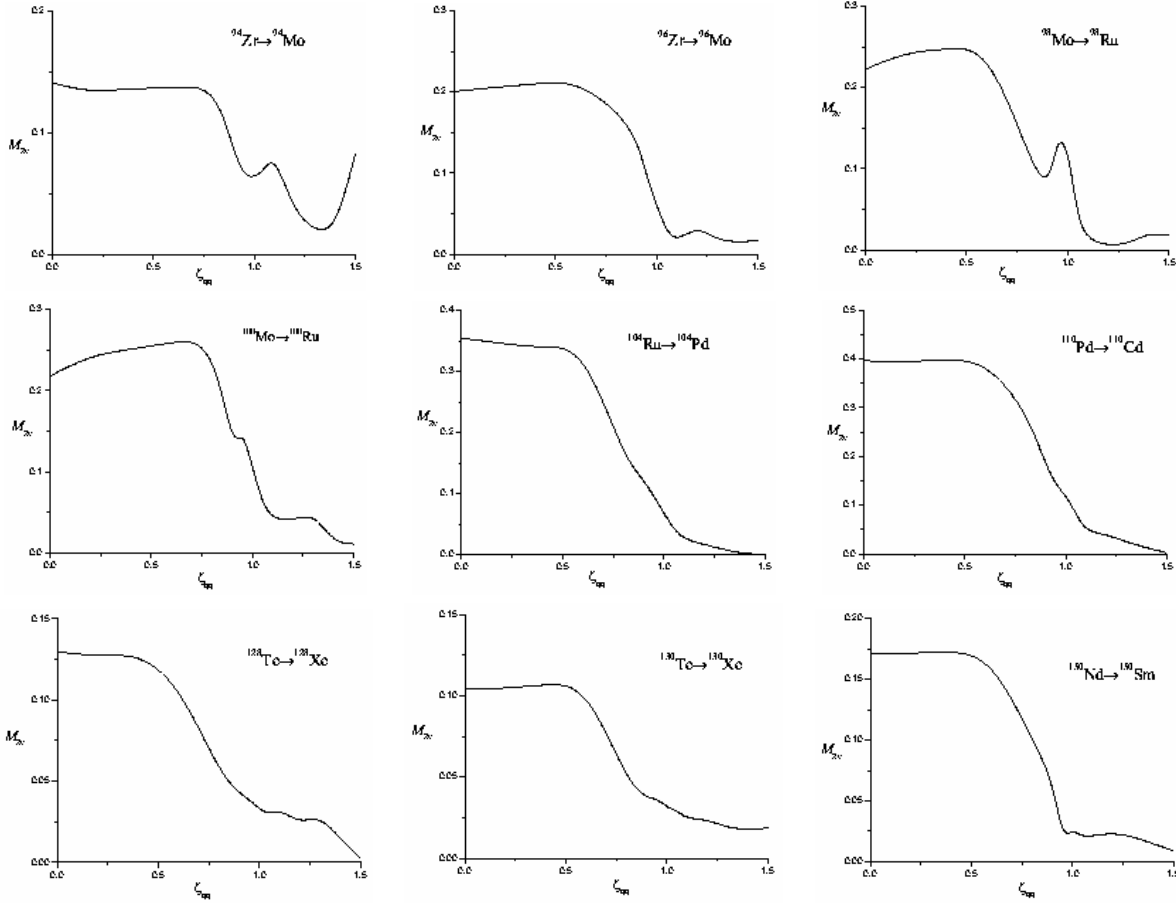


**Figure 1.** Dependence of  $M_{2\nu}$  on the strength of the  $QQHH$  interaction  $\zeta_{qq}$ .

To quantify the deformation effect on  $M_{2\nu}$ , we define a quantity  $D_{2\nu}$  as the ratio of  $M_{2\nu}$  at zero deformation ( $\zeta_{qq} = 0$ ) and full deformation ( $\zeta_{qq} = 1$ ). This ratio of deformation effect  $D_{2\nu}$  is given by

$$D_{2\nu} = \frac{M_{2\nu}(\zeta_{qq} = 0)}{M_{2\nu}(\zeta_{qq} = 1)} \quad (28)$$

The values of  $D_{2\nu}$  for  $^{94,96}\text{Zr}$ ,  $^{98,100}\text{Mo}$ ,  $^{104}\text{Ru}$ ,  $^{110}\text{Pd}$ ,  $^{128,130}\text{Te}$  and  $^{150}\text{Nd}$  nuclei for  $PQQHH(PQQ)$  type of effective two-body interaction are 2.23(2.29), 3.38(3.70), 1.75(1.86), 2.09(2.33), 5.19(5.47), 3.30(3.14), 3.97(4.26), 3.31(2.89) and 6.46(5.94) respectively. These values of  $D_{2\nu}$  suggest that the  $M_{2\nu}$  is quenched by a factor of approximately 2 to 6.5 in the mass range  $A = 90 - 150$  due to deformation effects. Further, the quenching is of almost same magnitude in the calculation using both type of effective two-body interaction. We like to mention here that in view of the limitations of the PHFB model as mentioned, the deformation effect for nuclei like  $^{94}\text{Zr}$  and  $^{96}\text{Zr}$  may be taken as a conservative estimate.

#### 4. Conclusions

To summarize, we employ the PHFB model using  $PQQHH$  type of effective two-body interaction to construct the yrast band wave functions of  $\beta\beta$  emitters. The overall agreement between the calculated and observed yrast spectra as well as electromagnetic properties of the nuclei suggests that the PHFB wave functions generated by fixing  $\chi_{2pn}$  to reproduce the  $E_{2+}$  are quite reliable. Subsequently, we employ the same wave functions to study the  $(\beta^-\beta^-)_{2\nu}$  decay of  $^{94,96}\text{Zr}$ ,  $^{98,100}\text{Mo}$ ,  $^{104}\text{Ru}$ ,  $^{110}\text{Pd}$ ,  $^{128,130}\text{Te}$  and  $^{150}\text{Nd}$  nuclei for the  $0^+ \rightarrow 0^+$  transition. The theoretically calculated NTMEs  $M_{2\nu}$  are compared with those extracted from experimentally observed half-lives  $T_{1/2}^{2\nu}$ . The agreement between the theoretically calculated results and experimentally observed data is quite satisfactory. We also examine the effect of deformation on NTMEs  $M_{2\nu}$  by varying the strength of  $QQHH$  part of the effective two-body interaction. It is noticed that the desired quenching of  $M_{2\nu}$  is achieved in the PHFB model through the subtle interplay of pairing and deformation degrees of freedom. Further, the results calculated with  $PQQ$  and  $PQQHH$  type of effective two-body interactions are quite similar, which underlines the stability of our previous results [41, 43].

Further, a reasonable agreement between the calculated and observed spectroscopic properties and  $M_{2\nu}$  of  $(\beta^-\beta^-)_{2\nu}$  decay for the  $0^+ \rightarrow 0^+$  transition of considered nuclei makes us confident to employ the same PHFB wave functions to study the  $(\beta^-\beta^-)_{0\nu}$  decay of the same nuclei, which will be reported soon.

This work was partially supported by DAE-BRNS, India vide sanction No. 2003/37/14/BRNS/669, by Conacyt-Mexico and DGAPA-UNAM.

- [1] Goepfert-Mayer M 1935 *Phys. Rev.* **48** 512
- [2] Fury W 1939 *Phys. Rev.* **56** 1184
- [3] Chikashige Y, Mohapatra R N and Peccei R D 1981 *Phys. Rev. Lett.* **45** 1926; 1981 *Phys. Lett. B* **98** 265
- [4] Aulakh C S and Mohapatra R N 1982 *Phys. Lett. B* **119** 136
- [5] Bamert P, Burgess C P and Mohapatra R N 1995 *Nucl. Phys. B* **449** 25
- [6] Rosen S P and Primakoff H 1959 *Report Prog. in Phys.* **22** 121
- [7] Bryman D and Picciotto C 1978 *Rev. Mod. Phys.* **50** 11
- [8] Primakoff H and Rosen S P 1981 *Ann. Rev. Nucl. Part. Sci.* **31** 145
- [9] Haxton W C, Stephenson G J Jr. 1984 *Prog. Part. Nucl. Phys.* **12** 409
- [10] Doi M, Kotani T and Takasugi E 1985 *Prog. Theo. Phys. Suppl.* **83** 1; Doi M and Kotani T 1992 *Prog. Theor. Phys.* **87** 1207; Doi M and Kotani T 1993 *Prog. Theor. Phys.* **89** 139
- [11] Vergados J D 1983 *Nucl. Phys. B* **218** 109; 2002 *Phys. Rep.* **133** 1; 2002 *ibid* **361** 1
- [12] Faessler A 1988 *Prog. Part. Nucl. Phys.* **21** 183
- [13] Tomoda T 1991 *Rep. Prog. Phys.* **54** 53
- [14] Boehm F and Vogel P 1984 *Ann. Rev. Nucl. Part. Sci.* **34**, 125; 1992 *Physics of Massive Neutrinos*, 2nd ed. (Cambridge University Press, Cambridge 1992).
- [15] Moe M K and Vogel P 1994 *Ann. Rev. Nucl. Part. Sci.* **44** 247
- [16] Zuber K 1998 *Phys. Rep.* **305** 295
- [17] Fiorini E 1998 *Phys. Rep.* **307** 309
- [18] Suhonen J and Civitarese O 1998 *Phys. Rep.* **300** 123
- [19] Faessler A and Simkovic F 1998 *J. Phys. G* **24** 2139
- [20] Ejiri H 2000 *Phys. Rep.* **338** 265
- [21] Klapdor-Kleingrothaus H V 2001 *Sixty years of Double Beta Decay*, World Scientific, Singapore
- [22] Elliott S R and Vogel P 2002 *Ann. Rev. Nucl. Part. Sci.* **52** 115
- [23] Elliott S R and Engel J 2004 *J. Phys. G* **30** R183
- [24] Tretyak V I and Zdesenko Y G 1995 *At. Data Nucl. Data Tables* **61** 43; 2002 *ibid* **80** 83
- [25] Caurier E, Nowacki F, Poves A and Retamosa J 1999 *Nucl. Phys. A* **654** 973
- [26] Caurier E, Nowacki F, Poves A and Retamosa J 1996 *Phys. Rev. Lett.* **77** 1954
- [27] Vogel P and Zirnbauer M R 1986 *Phys. Rev. Lett.* **57** 3148
- [28] Barabash A S 2006 *Czech. J. Phys.* **56** 437
- [29] Klapdor-Kleingrothaus H V, Krivosheina I V, Dietz A and Chkvorets O 2004 *Phys. Lett. B* **586** 198; Klapdor-Kleingrothaus H V *et al* 2001 *Mod. Phys. Lett. A* **16** 2409; 2001 *Eur. Phys. J. A* **12** 147
- [30] Aalseth C E *et al* 2002 *Phys. Rev. D* **65** 092007; 2002 *Mod. Phys. Lett. A* **17** 1475
- [31] Griffiths A and Vogel P 1992 *Phys. Rev. C* **46** 181
- [32] Suhonen J and Civitarese O 1994 *Phys. Rec. C* **49** 3055
- [33] Auerbach N, Zheng D C, Zamick L and Brown B A 1993 *Phys. Lett. B* **304** 17; Auerbach N, Bertsch G F, Brown B A and Zhao L 1993 *Nucl. Phys. A* **56** 190
- [34] Troltenier D, Draayer J P and Hirsch J G 1996 *Nucl. Phys. A* **601** 89
- [35] Frisk F, Hamamoto I and Zhang X Z 1995 *Phys. Rev. C* **52** 2468

- [36] Sarriguren P, Moya de Guerra E, Escuderos A and Carrizo A C 1998 *Nucl. Phys. A* **635** 55; Sarriguren P, Moya de Guerra E and Escuderos A 1999 *Nucl. Phys. A* **658** 13; *ibid* 2001 *Nucl. Phys. A* **691** 631
- [37] Náchter E *et al* 2004 *Phys. Rev. Lett.* **92** 232501
- [38] Álvarez-Rodríguez R, Sarriguren P, Moya de Guerra E, Pacearescu L, Faessler A and Simkovic F 2004 *Phys. Rev. C* **70** 064309
- [39] Pacearescu L, Faessler A and Simkovic F 2004 *Phys. At. Nucl.* **67** 1210
- [40] Baranger M and Kumar K 1968 *Nucl. Phys. A* **110** 490
- [41] Chandra R, Singh J, Rath P K, Raina P K and Hirsch J G 2005 *Eur. Phys. J. A* **23** 223
- [42] Raina P K, Shukla A, Singh S, Rath P K and Hirsch J G 2006 *Eur. Phys. J. A* **28** 27; Shukla A, Raina P K, Chandra R, Rath P K and Hirsch J G 2005 *Eur. Phys. J. A* **23** 235
- [43] Singh S, Chandra R, Rath P K, Raina P K and Hirsch J G 2007 *Eur. Phys. J. A* **33** 375
- [44] Sawhney N, Bharti A and Khosa S K 2002 *Pramana* **59** 585; War T A, Chandan A, Devi R, Khosa S K and Bharti A 2003 *Indian Journal of Pure & Applied Physics* **41** 914; War T A, Chandan A, Devi R, Bharti A and Khosa S K 2003 *Indian J. Phys.* **77A** 465; Chandan A, War T A, Sawhney N, Bharti A and Khosa S K 2004 *Indian J. Phys.* **78** 965
- [45] Dixit B M, Rath P K, Raina P K 2002 *Phys. Rev. C* **65** 034311; 2003 *ibid* **67** 059901(E)
- [46] Civitarese O and Suhonen J 1993 *Phys. Rev. C* **47** 2410
- [47] Bohr A and Mottelson B R 1998 *Nuclear Structure Vol. I (World Scientific, Singapore)*
- [48] Castaños O, Hirsch J G, Civitarese O and Hess P O 1994 *Nucl. Phys. A* **571** 276
- [49] Hirsch J G, Castaños O, Hess P O, Civitarese O 1995 *Phys. Rev. C* **51** 2252
- [50] Ceron V E and Hirsch J G 1999 *Phys. Lett. B* **471** 1
- [51] Onishi N and Yoshida S 1966 *Nucl. Phys. A* **260** 226
- [52] Heestand G M, Borchers R R, Herskind B, Grodzins L, Kalish R and Murnick D E 1969 *Nucl. Phys. A* **133** 310
- [53] Greiner W 1966 *Nucl. Phys.* **80** 417
- [54] Arima A 1981 *Nucl. Phys. A* **354** 19
- [55] Bohr A and Mottelson B R 1975 *Nuclear Structure Vol. II p. 356 (New York, Benjamin)*
- [56] Sakai M 1984 *At. Data, Nucl. Data Tables* **31** 400
- [57] Khosa S K, Tripathi P N and Sharma S K 1982 *Phys. Lett. B* **119** 257; Tripathi P N, Sharma S K and Khosa S K 1984 *Phys. Rev. C* **29** 1951; Sharma S K, Tripathi P N and Khosa S K 1988 *Phys. Rev. C* **38** 2935
- [58] Raman S, Malarkey C H, Milner W T, Nestor C W Jr. and Stelson P H 1987 *At. Data Nucl. Data Tables* **36** 1
- [59] Raman S, Nestor C W Jr. and Tikkanen P 2001 *At. Data Nucl. Data Tables* **78** 1
- [60] Raghavan P 1989 *At. Data Nucl. Data Table* **42** 189
- [61] Speidel K H, Kenn O and Nowacki F 2002 *Prog. Part. Nucl. Phys.* **49** 91
- [62] Arnold R *et al* 1999 *Nucl. Phys. A* **658** 299
- [63] Bobyk A, Kaminski W A and Zareba P 2000 *Nucl. Phys. A* **669** 221
- [64] Hirsch M, Wu X R, Klapdor-Kleingrothaus H V, Cheng-rui Ching and Tso-hsiu Ho 1994 *Phys. Rep.* **242** 403
- [65] Staudt A, Muto K and Klapdor-Kleingrothaus H V 1990 *Europhys. Lett.* **13** 31
- [66] Lalanne D, hep-ex/0509005
- [67] Wieser M E and De Laeter John R 2001 *Phys. Rev. C* **64** 024308
- [68] Barabash A S 1998 *Nucl. Phys. A* **629** 517c
- [69] Kawashima A, Takahashi K and Masuda A 1993 *Phys. Rev. C* **47** 2452
- [70] Rumyantsev O A and Urin M H 1998 *Phys. Lett. B* **443** 51
- [71] Toivanen J and Suhonen J 1997 *Phys. Rev. C* **55** 2314
- [72] Barbash A S, Gurriaran R, Hubert F, Hubert Ph, Reyss J L, Suhonen J and Umatov V I 1996 *J. Phys. G* **22** 487
- [73] Stoica S 1995 *Phys. Lett. B* **350** 152
- [74] Engel J, Vogel P, Zirnbauer M R 1988 *Phys. Rev. C* **37** 731
- [75] Arnold R *et al* 2005 *Phys. Rev. Lett.* **95** 182302
- [76] Hidaka H, Ly Chi V and Suzuki K 2004 *Phys. Rev. C* **70** 025501
- [77] Ashitkov V D *et al* 2001 *JETP Lett.* **74** 529
- [78] De Silva A, Moe M K, Nelson M A and Vient M A 1997 *Phys. Rev. C* **56** 2451
- [79] Alston Garnjost M *et al* 1997 *Phys. Rev. C* **55** 474
- [80] Dassie D *et al* (NEMO collaboration) 1995 *Phys. Rev. D* **51** 2090
- [81] Garcia A *et al* 1993 *Phys. Rev. C* **47** 2910
- [82] Ejiri H *et al* 1991 *J. Phys. G* **17** 155
- [83] Elliott S R, Moe M K, Nelson M A and Vient M A 1991 *J. Phys. G* **17** S145
- [84] Vasilev S I *et al* 1990 *JETP Lett.* **51** 622; 1993 *ibid* **58** 178
- [85] Simkovic F, Domin P and Semenov S V 2001 *J. Phys. G* **27** 2233
- [86] Civitarese O and Suhonen J 1998 *Phys. Rev. C* **58** 1535
- [87] Winter R G 1952 *Phys. Rev.* **85** 687
- [88] Semenov S V, Simkovic F, Khruschev V V and Domin P 2000 *Phys. At. Nucl.* **63** 1196
- [89] Stoica S 1994 *Phys. Rev. C* **49** 2240
- [90] Takaoka N *et al* 1996 *Phys. Rev. C* **53** 1557
- [91] Bernatovicz T, Brannon J, Brazzle R, Cowsik R, Hohenberg C and Podosek F 1992 *Phys. Rev. Lett.* **69** 2341; 1993 *Phys. Rev. C* **47** 806
- [92] Manuel O K 1991 *J. Phys. G* **17** S221

- [93] Lin J W *et al* 1988 *Nucl. Phys. A* **481** 484
- [94] Manuel O K 1986 *Proc. Int. Symp. on Nuclear Beta Decays, Neutrino, Osaka, Japan, June 1986 (World Sci., 1986)*,  
pg. 71
- [95] Aunola M and Suhonen J 1996 *Nucl. Phys. A* **602** 133
- [96] Scholten O and Yu Z R 1985 *Phys. Lett.* **161B** 13
- [97] Arnaboldi C *et al* 2003 *Phys. Lett. B* **557** 167
- [98] Rumyantsev O A and Urin M H 1995 *JETP Lett.* **61** 361
- [99] Artemiev V *et al* 1995 *Phys. Lett. B* **345** 564
- [100] Artemiev V *et al* 1993 *JETP Lett.* **58** 262

**Table 1:** Excitation energies  $E_{J^\pi}$  (MeV) of  $J^\pi = 2^+, 4^+$  and  $6^+$  yrast states of  $^{94,96}\text{Zr}$ ,  $^{94,96,98,100}\text{Mo}$ ,  $^{98,100,104}\text{Ru}$ ,  $^{104,110}\text{Pd}$ ,  $^{110}\text{Cd}$ ,  $^{128,130}\text{Te}$ ,  $^{128,130}\text{Xe}$ ,  $^{150}\text{Nd}$  and  $^{150}\text{Sm}$  nuclei.

Nucleus	$PQQ$	$PQQHH$	Exp.[56]	Nucleus	$PQQ$	$PQQHH$	Exp.[56]		
$^{94}\text{Zr}$	$\chi_{2pn}$	0.02519	0.02629	$^{94}\text{Mo}$	$\chi_{2pn}$	0.02670	0.02572		
	$E_{2^+}$	0.9182	0.9165		0.9183	$E_{2^+}$	0.8715	0.8713	0.871099
	$E_{4^+}$	1.9732	1.9657		1.4688	$E_{4^+}$	1.9685	1.9682	1.573726
	$E_{6^+}$	2.7993	2.8087			$E_{6^+}$	3.3136	3.3283	2.42337
$^{96}\text{Zr}$	$\chi_{2pn}$	0.01717	0.01918	$^{96}\text{Mo}$	$\chi_{2pn}$	0.02557	0.02472		
	$E_{2^+}$	1.7570	1.7541		1.7507	$E_{2^+}$	0.7779	0.7817	0.77821
	$E_{4^+}$	3.5269	3.6296		3.1202	$E_{4^+}$	2.0373	2.0220	1.62815
	$E_{6^+}$	9.7261	9.3686			$E_{6^+}$	3.5776	3.5300	2.44064
$^{98}\text{Mo}$	$\chi_{2pn}$	0.01955	0.01955	$^{98}\text{Ru}$	$\chi_{2pn}$	0.02763	0.02649		
	$E_{2^+}$	0.7892	0.7887		0.78742	$E_{2^+}$	0.6513	0.6522	0.65241
	$E_{4^+}$	1.9522	1.9916		1.51013	$E_{4^+}$	1.9430	1.9470	1.3978
	$E_{6^+}$	3.3098	3.4051		2.3438	$E_{6^+}$	3.6548	3.6703	2.2227
$^{100}\text{Mo}$	$\chi_{2pn}$	0.01906	0.01876	$^{100}\text{Ru}$	$\chi_{2pn}$	0.01838	0.01831		
	$E_{2^+}$	0.5356	0.5357		0.5355	$E_{2^+}$	0.5395	0.5402	0.5396
	$E_{4^+}$	1.4719	1.4766		1.1359	$E_{4^+}$	1.5591	1.5847	1.2265
	$E_{6^+}$	2.6738	2.6893			$E_{6^+}$	2.8940	2.9629	2.0777
$^{104}\text{Ru}$	$\chi_{2pn}$	0.02110	0.02053	$^{104}\text{Pd}$	$\chi_{2pn}$	0.01486	0.01507		
	$E_{2^+}$	0.3580	0.3578		0.35799	$E_{2^+}$	0.5552	0.5560	0.55579
	$E_{4^+}$	1.1339	1.1385		0.8885	$E_{4^+}$	1.5729	1.6138	1.32359
	$E_{6^+}$	2.2280	2.2486		1.5563	$E_{6^+}$	2.8790	2.9954	2.2498
$^{110}\text{Pd}$	$\chi_{2pn}$	0.01417	0.01393	$^{110}\text{Cd}$	$\chi_{2pn}$	0.01412	0.01414		
	$E_{2^+}$	0.3737	0.3738		0.3738	$E_{2^+}$	0.6576	0.6585	0.6577
	$E_{4^+}$	1.1563	1.1583		0.9208	$E_{4^+}$	1.8709	1.8921	1.5424
	$E_{6^+}$	2.2254	2.2359		1.5739	$E_{6^+}$	3.3865	3.4728	2.4799
$^{128}\text{Te}$	$\chi_{2pn}$	0.02715	0.02692	$^{128}\text{Xe}$	$\chi_{2pn}$	0.0360	0.02662		
	$E_{2^+}$	0.7436	0.7435		0.7432	$E_{2^+}$	0.4511	0.4420	0.4429
	$E_{4^+}$	2.0458	2.0130		1.4971	$E_{4^+}$	1.4263	1.3444	1.0329
	$E_{6^+}$	3.7363	3.6647		1.8111	$E_{6^+}$	2.7976	2.5404	1.7370
$^{130}\text{Te}$	$\chi_{2pn}$	0.01801	0.01890	$^{130}\text{Xe}$	$\chi_{2pn}$	0.02454	0.02281		
	$E_{2^+}$	0.8393	0.8395		0.8395	$E_{2^+}$	0.5385	0.5384	0.5361
	$E_{4^+}$	1.7741	1.8085		1.6325	$E_{4^+}$	1.5496	1.5268	1.2046
	$E_{6^+}$	3.0833	3.1283		1.8145	$E_{6^+}$	2.7831	2.7400	1.9444
$^{150}\text{Nd}$	$\chi_{2pn}$	0.02160	0.02228	$^{150}\text{Sm}$	$\chi_{2pn}$	0.01745	0.01730		
	$E_{2^+}$	0.1307	0.1300		0.13012	$E_{2^+}$	0.3328	0.3359	0.33395
	$E_{4^+}$	0.4320	0.4305		0.3815	$E_{4^+}$	1.0156	1.0290	0.77335
	$E_{6^+}$	0.8960	0.8958			$E_{6^+}$	1.9185	1.9504	1.27885

**Table 2:** Comparison of calculated and experimentally observed reduced transition probabilities  $B(E2:0^+ \rightarrow 2^+)$ , static quadrupole moments  $Q(2^+)$  and  $g$ -factors  $g(2^+)$  of  $^{94,96}\text{Zr}$ ,  $^{94,96,98,100}\text{Mo}$ ,  $^{98,100,104}\text{Ru}$ ,  $^{104,110}\text{Pd}$ ,  $^{110}\text{Cd}$ ,  $^{128,130}\text{Te}$ ,  $^{128,130}\text{Xe}$ ,  $^{150}\text{Nd}$  and  $^{150}\text{Sm}$  nuclei. Here  $B(E2)$  and  $Q(2^+)$  are calculated for effective charge  $e_p = 1 + e_{eff}$  and  $e_n = e_{eff}$ . Here  $\dagger$  and  $\ddagger$  denote the calculation with  $PQQHH$  and  $PQQ$  type of effective two-body interaction respectively.

Nucleus	$B(E2:0^+ \rightarrow 2^+) (e^2b^2)$				$Q(2^+) (eb)$			$g(2^+) (nm)$					
	Theory		Exp.[58]		Theory		Exp.[60]	Theory	Exp.[60]				
	$e_{eff}$				$e_{eff}$								
	0.40	0.50	0.60	0.40	0.50	0.60							
$^{94}\text{Zr}$	$\dagger$	0.056	0.075	<b>0.097</b>	0.066 $\pm$ 0.014*	$\dagger$	-0.207	-0.240	<b>-0.272</b>	$\dagger$	0.112	-0.329 $\pm$ 0.015 <sup>a</sup>	
	$\ddagger$	0.046	0.062	<b>0.081</b>	0.081 $\pm$ 0.017 0.056 $\pm$ 0.014	$\ddagger$	-0.168	-0.195	<b>-0.222</b>	$\ddagger$	0.121	-0.26 $\pm$ 0.06 -0.05 $\pm$ 0.05	
$^{94}\text{Mo}$	$\dagger$	0.148	0.187	<b>0.232</b>	0.203 $\pm$ 0.004*	$\dagger$	-0.347	-0.391	<b>-0.435</b>	-0.13 $\pm$ 0.08	$\dagger$	0.343	
	$\ddagger$	0.148	0.188	<b>0.232</b>	0.230 $\pm$ 0.040 0.270 $\pm$ 0.035	$\ddagger$	-0.347	-0.391	<b>-0.435</b>		$\ddagger$	0.343	
$^{96}\text{Zr}$	$\dagger$	0.046	<b>0.063</b>	0.081	0.055 $\pm$ 0.022*	$\dagger$	-0.009	<b>-0.011</b>	-0.014		$\dagger$	0.297	
	$\ddagger$	0.044	<b>0.060</b>	0.078		$\ddagger$	-0.012	<b>-0.015</b>	-0.018		$\ddagger$	0.254	
$^{96}\text{Mo}$	$\dagger$	0.250	<b>0.317</b>	0.391	0.271 $\pm$ 0.005*	$\dagger$	-0.453	<b>-0.509</b>	-0.566	-0.20 $\pm$ 0.08	$\dagger$	0.535	
	$\ddagger$	0.265	<b>0.335</b>	0.413	0.310 $\pm$ 0.047 0.302 $\pm$ 0.039	$\ddagger$	-0.466	<b>-0.524</b>	-0.582		$\ddagger$	0.563	
$^{98}\text{Mo}$	$\dagger$	<b>0.246</b>	0.316	0.395	0.267 $\pm$ 0.009*	$\dagger$	<b>-0.450</b>	-0.510	-0.570	-0.26 $\pm$ 0.09	$\dagger$	0.405	0.34 $\pm$ 0.18
	$\ddagger$	<b>0.234</b>	0.302	0.378	0.259 $\pm$ 0.010 0.260 $\pm$ 0.040	$\ddagger$	<b>-0.439</b>	-0.498	-0.557		$\ddagger$	0.376	
$^{98}\text{Ru}$	$\dagger$	<b>0.389</b>	0.488	0.599	0.392 $\pm$ 0.012*	$\dagger$	<b>-0.565</b>	-0.633	-0.700	-0.20 $\pm$ 0.09	$\dagger$	0.510	0.39 $\pm$ 0.30
	$\ddagger$	<b>0.433</b>	0.543	0.665	0.411 $\pm$ 0.035 0.475 $\pm$ 0.038	$\ddagger$	<b>-0.596</b>	-0.667	-0.739	-0.03 $\pm$ 0.14	$\ddagger$	0.528	
$^{100}\text{Mo}$	$\dagger$	0.306	0.394	<b>0.493</b>	0.516 $\pm$ 0.010*	$\dagger$	-0.500	-0.567	<b>-0.635</b>	-0.42 $\pm$ 0.09	$\dagger$	0.467	0.34 $\pm$ 0.18
	$\ddagger$	0.320	0.412	<b>0.515</b>	0.511 $\pm$ 0.009 0.526 $\pm$ 0.026	$\ddagger$	-0.512	-0.581	<b>-0.650</b>	-0.39 $\pm$ 0.08	$\ddagger$	0.477	
$^{100}\text{Ru}$	$\dagger$	0.306	0.390	<b>0.484</b>	0.490 $\pm$ 0.005*	$\dagger$	-0.501	-0.565	<b>-0.630</b>	-0.54 $\pm$ 0.07	$\dagger$	0.363	0.47 $\pm$ 0.06
	$\ddagger$	0.308	0.393	<b>0.488</b>	0.493 $\pm$ 0.003 0.494 $\pm$ 0.006	$\ddagger$	-0.503	-0.568	<b>-0.633</b>	-0.40 $\pm$ 0.12 -0.43 $\pm$ 0.07	$\ddagger$	0.355	0.51 $\pm$ 0.07
$^{104}\text{Ru}$	$\dagger$	0.558	0.714	<b>0.890</b>	0.820 $\pm$ 0.012*	$\dagger$	-0.676	-0.765	<b>-0.854</b>	-0.76 $\pm$ 0.19	$\dagger$	0.345	0.41 $\pm$ 0.05
	$\ddagger$	0.572	0.732	<b>0.912</b>	0.93 $\pm$ 0.06 1.04 $\pm$ 0.16	$\ddagger$	-0.684	-0.774	<b>-0.864</b>	-0.70 $\pm$ 0.08 -0.66 $\pm$ 0.05	$\ddagger$	0.339	

Table 2 continued

Nucleus	$B(E2:0^+ \rightarrow 2^+) (e^2b^2)$				$Q(2^+) (eb)$			$g(2^+) (nm)$					
	Theory			Exp.[58]	Theory			Exp.[60]	Theory				
	$e_{eff}$				$e_{eff}$				Theory	Exp.[60]			
	0.40	0.50	0.60	0.40	0.50	0.60							
$^{104}\text{Pd}$	†	0.371	0.473	<b>0.586</b>	$0.535 \pm 0.035^*$	†	-0.550	-0.621	<b>-0.692</b>	$-0.47 \pm 0.10$	†	0.458	$0.46 \pm 0.04$
	‡	0.361	0.460	<b>0.571</b>	$0.61 \pm 0.09$ $0.535 \pm 0.035$	‡	-0.543	-0.613	<b>-0.682</b>		‡	0.439	$0.40 \pm 0.05$ $0.38 \pm 0.04$
$^{110}\text{Pd}$	†	0.471	<b>0.604</b>	0.754	$0.870 \pm 0.040^*$	†	-0.620	<b>-0.702</b>	-0.784	$-0.72 \pm 0.14$	†	0.489	$0.37 \pm 0.03$
	‡	0.479	<b>0.614</b>	0.766	$0.780 \pm 0.120$ $0.820 \pm 0.080$	‡	-0.626	<b>-0.708</b>	-0.791	$-0.55 \pm 0.08$ $-0.47 \pm 0.03$	‡	0.478	$0.35 \pm 0.03$
$^{110}\text{Cd}$	†	0.407	<b>0.522</b>	0.653	$0.450 \pm 0.020^*$	†	-0.575	<b>-0.651</b>	-0.728	$-0.40 \pm 0.04$	†	0.377	$0.31 \pm 0.07$
	‡	0.427	<b>0.548</b>	0.685	$0.504 \pm 0.040$ $0.467 \pm 0.019$	‡	-0.590	<b>-0.668</b>	-0.746	$-0.39 \pm 0.05$ $-0.36 \pm 0.08$	‡	0.358	$0.285 \pm 0.055$
$^{128}\text{Te}$	†	0.300	<b>0.384</b>	0.479	$0.383 \pm 0.006^*$	†	-0.498	<b>-0.563</b>	-0.628	$-0.14 \pm 0.12$	†	0.526	$0.35 \pm 0.04$
	‡	0.298	<b>0.381</b>	0.474	$0.380 \pm 0.009$ $0.378 \pm 0.007$	‡	-0.496	<b>-0.561</b>	-0.626	$-0.06 \pm 0.05$	‡	0.514	$0.31 \pm 0.04$
$^{128}\text{Xe}$	†	0.571	<b>0.729</b>	0.906	$0.750 \pm 0.040^*$	†	-0.685	<b>-0.774</b>	-0.862		†	0.439	$0.41 \pm 0.07$
	‡	0.637	<b>0.819</b>	1.024	$0.790 \pm 0.040$ $0.890 \pm 0.230$	‡	-0.724	<b>-0.820</b>	-0.917		‡	0.400	$0.31 \pm 0.03$
$^{130}\text{Te}$	†	0.242	<b>0.304</b>	0.373	$0.295 \pm 0.007^*$	†	-0.448	<b>-0.502</b>	-0.556	$-0.15 \pm 0.10$	†	0.667	$0.33 \pm 0.08$
	‡	0.231	<b>0.289</b>	0.354	$0.290 \pm 0.011$ $0.260 \pm 0.050$	‡	-0.438	<b>-0.490</b>	-0.542		‡	0.679	$0.29 \pm 0.06$
$^{130}\text{Xe}$	†	0.478	<b>0.605</b>	0.746	$0.65 \pm 0.05^*$	†	-0.627	<b>-0.705</b>	-0.783		†	0.478	$0.38 \pm 0.07$
	‡	0.493	<b>0.624</b>	0.769	$0.631 \pm 0.048$ $0.640 \pm 0.160$	‡	-0.637	<b>-0.716</b>	-0.795		‡	0.463	$0.31 \pm 0.04$
$^{150}\text{Nd}$	†	2.172	<b>2.632</b>	3.136	$2.760 \pm 0.040^*$	†	-1.335	<b>-1.469</b>	-1.604	$-2.00 \pm 0.51$	†	0.622	$0.422 \pm 0.039$
	‡	2.132	<b>2.580</b>	3.070	$2.640 \pm 0.080$ $2.670 \pm 0.100$	‡	-1.322	<b>-1.455</b>	-1.587		‡	0.636	$0.322 \pm 0.009$
$^{150}\text{Sm}$	†	1.741	<b>2.098</b>	2.488	$1.350 \pm 0.030^*$	†	-1.193	<b>-1.310</b>	-1.426	$-1.32 \pm 0.19$	†	0.604	$0.385 \pm 0.027$
	‡	1.707	<b>2.056</b>	2.437	$1.470 \pm 0.090$ $1.440 \pm 0.150$	‡	-1.182	<b>-1.297</b>	-1.412	$-1.25 \pm 0.20$	‡	0.592	$0.411 \pm 0.032$

\*Average  $B(E2)$  values[59], <sup>a</sup>[61]

**Table 3:** Experimental half-life  $T_{1/2}^{2\nu}$  and corresponding NTME  $M_{2\nu}$  for the  $0^+ \rightarrow 0^+$  transition of  $^{94,96}\text{Zr}$ ,  $^{98,100}\text{Mo}$ ,  $^{104}\text{Ru}$ ,  $^{110}\text{Pd}$ ,  $^{128,130}\text{Te}$  and  $^{150}\text{Nd}$  nuclei along with theoretically calculated NTME  $M_{2\nu}$  and half-life  $T_{1/2}^{2\nu}$  in different nuclear models. The numbers corresponding to (a) and (b) are calculated for  $g_A = 1.25$  and  $1.0$  respectively. “gch.” denotes the geochemical experiment and “\*” denotes the present calculation.

Nuclei	Project	Experiment		$ M_{2\nu} $	Model	Ref.	Theory					
		Ref.	$T_{1/2}^{2\nu}$				$ M_{2\nu} $	$T_{1/2}^{2\nu}$				
$^{94}\text{Zr}$ ( $10^{22}$ yr)	NEMO 2	[62]	$>1.1 \times 10^{-5}$	(a)	$<62.815$	PHFB*	$PQQHH$	0.063	(a)	10.86		
				(b)	$<98.148$		$PQQ$	0.076	(b)	26.52		
	gch.	[67]	$0.94 \pm 0.32$	(a)	$0.074_{-0.0101}^{+0.0172}$	SRQRPA	[63]	$PQQ$	0.058	(a)	7.51	
				(b)	$0.116_{-0.0158}^{+0.0269}$					(b)	18.34	
				(a)	$0.051_{-0.012}^{+0.021}$					OEM	[64]	168
				(b)	$0.080_{-0.019}^{+0.033}$					QRPA	[65]	6.93
				(a)	$0.036_{-0.0036}^{+0.0051}$							
NEMO 2	[68]	$2.0_{-0.5}^{+0.9} \pm 0.5$	(a)	$0.051_{-0.012}^{+0.021}$	SRQRPA	[63]		0.059	(a)	1.47		
(b)	$0.080_{-0.019}^{+0.033}$	SU(4) $_{\sigma\tau}$	[70]	0.0678	(a)	1.13						
gch.	[69]	$3.9 \pm 0.9$	(a)	$0.036_{-0.0036}^{+0.0051}$				(b)	2.76			
(b)	$0.057_{-0.0056}^{+0.0080}$	RQRPA $^\dagger$	[71]			4.4						
Average Value	[22]	$1.4_{-0.5}^{+3.5}$	(a)	$0.061_{-0.0283}^{+0.0151}$	RQRPA $^\ddagger$	[71]				4.2		
(b)	$0.095_{-0.0443}^{+0.0235}$	QRPA	[72]	0.12-0.31	(a)	0.054-0.36						
Recommended Value	[28]	$2.0 \pm 0.3$	(a)	$0.051_{-0.0034}^{+0.0043}$				(b)	0.13-0.88			
(b)	$0.078_{-0.0054}^{+0.0067}$	SRPA	[73]	0.022	(a)	10.72						
			(b)	$0.078_{-0.0054}^{+0.0067}$				(b)	26.18			
					OEM	[64]				20.2		
					QRPA	[65]				1.08		
					QRPA	[74]	0.124		(a)	0.34		
									(b)	0.82		
$^{98}\text{Mo}$ ( $10^{29}$ yr)	PHFB*	$PQQHH$	0.127	(a)					(a)	6.36		
				(b)					(b)	15.52		
	SRQRPA	[63]	$PQQ$	0.130	(a)				(a)	6.09		
					(b)				(b)	14.87		
										4.06-15.2		
OEM	[64]								61.6			
QRPA	[65]								29.6			
$^{100}\text{Mo}$ ( $10^{18}$ yr)	NEMO 3	[75]	$7.11 \pm 0.02 \pm 0.54$	(a)	$0.122_{-0.0045}^{+0.0051}$	PHFB*	$PQQHH$	0.104	(a)	9.71		
				(b)	$0.191_{-0.0071}^{+0.0080}$				(b)	23.72		
	NEMO 3	[66]	$7.72 \pm 0.02 \pm 0.54$	(a)	$0.117_{-0.0040}^{+0.0045}$	SRQRPA	[63]	$PQQ$	0.104	(a)	9.79	
				(b)	$0.183_{-0.0063}^{+0.0070}$					(b)	23.90	
	gch.	[76]	$2.1 \pm 0.3$	(a)	$0.225_{-0.0145}^{+0.0180}$	SSDH	[85]			(a)	7.15-8.97	
				(b)	$0.351_{-0.0227}^{+0.0281}$					SRQRPA	[63]	5.04-16800

Table 3 continued

Nuclei	Project	Experiment		$ M_{2\nu} $	Model	Theory				
		Ref.	$T_{1/2}^{2\nu}$			Ref.	$ M_{2\nu} $	$T_{1/2}^{2\nu}$		
	ITEP+INFN	[77]	$7.2 \pm 0.9 \pm 1.8$	(a)	$0.121^{+0.0321}_{-0.0179}$	SU(4) $_{\sigma\tau}$	[70]	0.1606	(a)	4.11
				(b)	$0.190^{+0.0502}_{-0.0279}$				(b)	10.03
	UC Irvine	[78]	$6.82^{+0.38}_{-0.53} \pm 0.68$	(a)	$0.125^{+0.0128}_{-0.0087}$	SSDH	[86]	0.18	(a)	3.27
				(b)	$0.195^{+0.0200}_{-0.0136}$				(b)	7.99
	LBL+MHC+ UNM+INEL	[79]	$7.6^{+2.2}_{-1.4}$	(a)	$0.118^{+0.0127}_{-0.0141}$	SRPA	[73]	0.059	(a)	30.45
				(b)	$0.185^{+0.0198}_{-0.0220}$				(b)	74.34
	NEMO	[80]	$9.5 \pm 0.4 \pm 0.9$	(a)	$0.106^{+0.008}_{-0.007}$	pSU(3) $^+$	[49]	0.152	(a)	4.59
				(b)	$0.165^{+0.013}_{-0.010}$				(b)	11.2
	LBL	[81]	$9.7 \pm 4.9$	(a)	$0.105^{+0.0441}_{-0.0193}$	pSU(3) $^{++}$	[49]	0.108	(a)	9.09
				(b)	$0.163^{+0.0689}_{-0.0302}$				(b)	22.19
	ELEGANTS V	[82]	$11.5^{+3.0}_{-2.0}$	(a)	$0.096^{+0.0096}_{-0.0105}$	OEM	[64]			35.8
				(b)	$0.150^{+0.0150}_{-0.0164}$	QRPA	[32]	0.101	(a)	10.39
	UC Irvine	[83]	$11.6^{+3.4}_{-0.8}$	(a)	$0.096^{+0.0035}_{-0.0115}$				(b)	25.37
				(b)	$0.149^{+0.0054}_{-0.0180}$	QRPA	[31]	0.256	(a)	1.62
	INS Baksan	[84]	$3.3^{+2.0}_{-1.0}$	(a)	$0.179^{+0.0355}_{-0.0378}$				(b)	3.95
				(b)	$0.280^{+0.0554}_{-0.0591}$	QRPA	[65]			1.13
	Average Value	[22]	$8.0 \pm 0.6$	(a)	$0.115^{+0.0054}_{-0.0047}$	QRPA	[74]	0.211	(a)	2.38
				(b)	$0.180^{+0.0084}_{-0.0074}$				(b)	5.81
	Average Value	[28]	$7.1 \pm 0.4$	(a)	$0.122^{+0.0036}_{-0.0033}$					
				(b)	$0.191^{+0.0056}_{-0.0052}$					
$^{104}\text{Ru}$ ( $10^{22}$ yr)						PHFB*	<i>PQQHH</i>	0.068	(a)	2.35
									(b)	5.73
							<i>PQQ</i>	0.068	(a)	2.35
									(b)	5.73
						OEM	[64]			3.09
						QRPA	[65]			0.629
$^{110}\text{Pd}$ ( $10^{20}$ yr)		[87]	$>6.0 \times 10^{-4}$	(a)	$<6.468$	PHFB*	<i>PQQHH</i>	0.120	(a)	1.74
				(b)	$<10.106$				(b)	4.24
							<i>PQQ</i>	0.133	(a)	1.41
									(b)	3.44
						SSDH	[88]			1.6
						SSDH	[86]	0.19	(a)	0.7
									(b)	1.70
						SRPA	[89]	0.046	(a)	11.86
									(b)	28.96
						OEM	[64]			12.4
						QRPA	[65]			0.116

Table 3 continued

Nuclei	Project	Experiment			Theory						
		Ref.	$T_{1/2}^{2\nu}$		$ M_{2\nu} $	Model	Ref.	$ M_{2\nu} $	$T_{1/2}^{2\nu}$		
$^{128}\text{Te}$ ( $10^{24}$ yr)	gch.	[90]	$(2.2\pm 0.3)$	(a)	$0.023^{+0.0018}_{-0.0014}$	PHFB*	$PQQHH$	0.033	(a)	1.10	
				(b)	$0.036^{+0.0027}_{-0.0022}$				(b)	2.68	
	gch.	[91]	$7.7\pm 0.4$	(a)	$0.012^{+0.0003}_{-0.0003}$		$PQQ$	0.033	(a)	1.05	
				(b)	$0.019^{+0.0005}_{-0.0005}$				(b)	2.55	
	gch.	[92]	2.0	(a)	0.024	SSDH	[88]	0.048	(a)	0.51	
				(b)	0.038				(b)	1.29	
	gch.	[93]	$1.8\pm 0.7$	(a)	$0.026^{+0.0071}_{-0.0039}$	SM	[25]			0.5	
				(b)	$0.040^{+0.0111}_{-0.0060}$				SU(4) $_{\sigma\tau}$	[70]	0.053
	gch.	[94]	$1.4\pm 0.4$	(a)	$0.029^{+0.0053}_{-0.0034}$					(b)	1.06
				(b)	$0.045^{+0.0083}_{-0.0053}$				SSDH	[86]	0.013
	Average Value	[22]	$7.2\pm 0.3$	(a)	$0.013^{+0.0003}_{-0.0003}$					(b)	17.65
				(b)	$0.020^{+0.0004}_{-0.0004}$				MCM	[95]	0.046
	Recommended Value	[28]	$2.5\pm 0.4$	(a)	$0.022^{+0.0014}_{-0.0012}$					(b)	1.41
				(b)	$0.034^{+0.0022}_{-0.0019}$				SRPA	[89]	0.006
									(b)	82.87	
							OEM	[64]		0.21	
							QRPA	[65]		2.63	
							QRPA	[74]	0.074	(a)	0.22
									(b)	0.54	
						IBM	[96]		0.09		
						WCSM	[9]	0.120	(a)	0.08	
									(b)	0.21	
$^{130}\text{Te}$ ( $10^{20}$ yr)	Milano+INFN	[97]	$6.1\pm 1.4^{+2.9}_{-3.5}$	(a)	$0.018^{+0.0232}_{-0.0043}$	PHFB*	$PQQHH$	0.031	(a)	2.10	
				(b)	$0.029^{+0.0362}_{-0.0068}$				(b)	5.13	
	gch.	[90]	$7.9\pm 1.0$	(a)	$0.016^{+0.0011}_{-0.0009}$					(a)	1.16
				(b)	$0.025^{+0.0018}_{-0.0015}$				(b)	2.82	
	gch.	[91]	$27.0\pm 1.0$	(a)	$0.009^{+0.0002}_{-0.0002}$	SM	[25]	0.030	(a)	2.3	
				(b)	$0.014^{+0.0003}_{-0.0002}$				(b)	5.84	
	gch.	[93]	$7.5\pm 0.3$	(a)	$0.017^{+0.0003}_{-0.0003}$	SU(4) $_{\sigma\tau}$	[70]	0.0468	(a)	0.95	
				(b)	$0.026^{+0.0005}_{-0.0005}$				(b)	2.32	
	Average Value	[22]	$27\pm 1.0$	(a)	$0.009^{+0.0002}_{-0.0002}$		RQRPA $^\dagger$	[71]	0.009	(a)	25.68
				(b)	$0.014^{+0.0003}_{-0.0002}$					(b)	62.70
	Recommended Value	[28]	$9.0\pm 1.0$	(a)	$0.015^{+0.0009}_{-0.0008}$		RQRPA $^\ddagger$	[71]	0.009	(a)	25.68
				(b)	$0.024^{+0.0014}_{-0.0012}$					(b)	62.70
							MCM	[95]	0.028	(a)	2.65
										(b)	6.48
							SU(4) $_{\sigma\tau}$	[98]			7.0
							SRPA	[89]	0.016	(a)	8.12
										(b)	19.84
							OEM	[64]			0.79
						QRPA	[65]			18.4	
						QRPA	[74]	0.049	(a)	0.87	
									(b)	2.12	
						IBM	[96]			0.17	
						WCSM	[9]	0.114	(a)	0.16	
									(b)	0.40	

Table 3 continued

Nuclei	Project	Experiment			Theory					
		Ref.	$T_{1/2}^{2\nu}$		$ M_{2\nu} $	Model	Ref.	$ M_{2\nu} $	$T_{1/2}^{2\nu}$	
$^{150}\text{Nd}$ ( $10^{18}$ yr)	NEMO 3	[66]	$9.7 \pm 0.7 \pm 1.0$	(a)	$0.029^{+0.0030}_{-0.0023}$	PHFB*	$PQQHH$	0.027	(a)	11.95
				(b)	$0.046^{+0.0047}_{-0.0036}$				(b)	29.17
	UCI	[78]	$6.75^{+0.37}_{-0.42} \pm 0.68$	(a)	$0.035^{+0.0033}_{-0.0025}$	$SU(4)_{\sigma\tau}$	[70]	0.0642	(a)	2.04
				(b)	$0.055^{+0.0051}_{-0.0038}$				(b)	4.98
	ITEP +INR	[99]	$18.8^{+6.6}_{-3.9} \pm 1.9$	(a)	$0.021^{+0.0043}_{-0.0036}$	pSU(3)	[48]	0.055	(a)	2.78
				(b)	$0.033^{+0.0067}_{-0.0056}$				(b)	6.79
	ITEP +INR	[100]	$17^{+10}_{-5.0} \pm 3.5$	(a)	$0.022^{+0.0092}_{-0.0056}$	OEM	[64]			16.6
				(b)	$0.035^{+0.0144}_{-0.0088}$				QRPA	[65]
	Average Value	[22]	$7.0^{+11.8}_{-0.3}$	(a)	$0.035^{+0.0008}_{-0.0135}$					
	Average Value	[28]	$7.8 \pm 0.7$	(b)	$0.054^{+0.0012}_{-0.0211}$					
	Average Value			(a)	$0.033^{+0.0016}_{-0.0014}$					
	Average Value			(b)	$0.051^{+0.0025}_{-0.0022}$					

$^\dagger$ AWS basis;  $^\ddagger$ WS basis;  $^+$ Spherical occupation wave functions;  $^{++}$ Deformed occupation wave functions